


FIREURISK - DEVELOPING A HOLISTIC, RISK-WISE STRATEGY FOR EUROPEAN WILDFIRE MANAGEMENT

Grant Agreement Number: 101003890	Call identifier: H2020-LC-CLA-2018-2019-2020
Topic:	LC-CLA-15-2020: Forest Fires risk reduction: towards an integrated fire management approach in the E.U.
Instrument:	RIA

D3.1 – Downscaled CMIP5 and CMIP6 climate scenarios for selected PS and DA

Deliverable Identifier:	D3.1
Deliverable Due Date:	30/09/2022
Deliverable Submission Date:	30/09/2022
Deliverable Version:	v.1.0
Lead partner:	Meteogrid
Authors:	Meteogrid, NCSRD
Work Package:	WP3 - Adaptation to future fire regimes
Task:	Task 3.1.1 - Climate change scenario data.
Dissemination Level:	☐ PU: Public ☒ CO: Confidential, only for members of the Consortium (including the Commission Services)



This project has received funding from the European Union's Horizon 2020 research and innovation programme under grant agreement No 101003890.

Revision History

Version	Date	Edited by	Description
v.0.1	22/08/2022	Meteogrid	Document Content outline / structure
v.0.2	14/09/2022	Meteogrid	Draft version
v.0.3	14/09/2022	Meteogrid	Complete version formatted according to template
v.0.4	14/09/2022	Meteogrid	Complete version with Annexes
v.0.5	15/09/2022	Meteogrid	Complete draft review by WP3 Leader
v.0.6	27/09/2022	Meteogrid	Internal review of the Complete version
v.0.9	29/09/2022	Meteogrid	Internal approval review by the QRB
v.1.0	30/09/2022	Meteogrid	Final version submitted

Quality Control

Type	Date	Reviewed by	Approved/Comment
Internal review	26/09/2022	Peter Verburg	Minor changes suggested
Internal review	29/09/2022	Vasileios Kazoukas	Approved

Copyright © FirEURisk Consortium. All rights reserved.

Executive Summary

The main objective of this deliverable is to provide a description of the methods and results concerning the climate projections generated under the Task 3.1.1 - “Climate change scenario data”. It includes the variables that most influence fire risk with a final resolution grid of 1km in each study area and of 9 km for the whole European domain. To achieve this objective, we used a methodology consisting on transference functions applied to CMIP6 climate models, trained with data from past reanalyses. Therefore, taking each reanalysis grid point (9 km resolution) as a reference, it has been possible to downscale the entire projected daily series (without forcing the seasonal variability) of all the models and scenarios for all the climate variables necessary to determine fire risk. These corrected downscaled projections have been obtained for a grid covering all European countries, with a good performance in the seasonal cycle over the year, for all the cases. Once the projections for the European grid were obtained, the Drought Code was calculated for each Pilot Site and Demonstration Area and, subsequently, three projections (models + scenarios combination) were selected according to their Drought Code difference between the beginning and the end of the 21st Century. Finally these climate projections of all the variables needed have been downscaled to a 1km grid in the Pilot Sites and Demonstration Areas. Both the projections of the 9km European grid and the projections of the 1km grid for PS/DA have been subjected to an exhaustive validation process, having obtained excellent results. All the data is available by an OpenDAP server.

Copyright © FirEURisk Consortium. All rights reserved.

Disclaimer

The content of the publication herein is the sole responsibility of the publishers and it does not necessarily represent the views expressed by the European Commission or its services.

While the information contained in the documents is believed to be accurate, the authors(s) or any other participant in the FirEURisk consortium make no warranty of any kind with regard to this material including, but not limited to the implied warranties of merchantability and fitness for a particular purpose.

Neither the FirEurisk Consortium nor any of its members, their officers, employees or agents shall be responsible or liable in negligence or otherwise howsoever in respect of any inaccuracy or omission herein.

Without derogating from the generality of the foregoing neither the FirEurisk Consortium nor any of its members, their officers, employees or agents shall be liable for any direct or indirect or consequential loss or damage caused by or arising from any information advice or inaccuracy or omission herein.

Copyright message

© FirEURisk Consortium, 2021-2025. This deliverable contains original unpublished work except where clearly indicated otherwise. Acknowledgement of previously published material and of the work of others has been made through appropriate citation, quotation or both. Reproduction is authorised provided the source is acknowledged.

Copyright © FirEURisk Consortium. All rights reserved.

Table of Contents

Introduction **10**

Purpose 10

State of the art 10

Structure of the report 10

Study area and data **11**

Study area: Demonstration Areas (DA) and Pilot Sites (PS) 11

Atmospheric reanalysis: ERA5-Land 12

Earth System Models: CMIP5 and CMIP6 experiments 15

Methodology **17**

CMIP6 downscaling to 0.07°×0.07° resolution grid 17

CMIP6 downscaling to 1km x 1km resolution grid 20

CMIP5 contrast experiment in MED-Greece 20

Results, products and validation **24**

CMIP6 downscaling to 0.07°×0.07° resolution grid 24

CMIP6 downscaling to 1km x 1km resolution grid 26

CMIP5 contrast experiment in MED-Greece 32

Documentation of results 35

Conclusions **36**

References **37**

Annex A: Climate scenarios of the MED-Greece experiments **39**

Annex B: Selection of climate models and scenarios **44**

Copyright © FirEURisk Consortium. All rights reserved.

List of Figures

Figure 1: Study area of FirEURisk, with borders in {32°N, 72°N; 15°W, 35°E} and location of the Demonstration Areas and Pilot Sites. 11

Figure 2: Validation of the daily surface fields simulated by ERA5-Land: Pearson correlation between observations and simulations for (a) maximum temperature, (b) mean wind and (c) total precipitation for Valencia (left) and for a set of ten reference observatories in Europe (right). 14

Figure 3: Comparison between the scenarios defined under CMIP6 and those defined under CMIP5. Tier 1 and Tier 2 are defined as those scenarios which are to be provided on an obligatory and optional basis, respectively, by all the climate models which form part of each phase of the CMPI. 15

Figure 4: Example downscaling processes of a daily field output from CMIP6 Earth System Models, applying transfer functions: a) Original gridded model output of a particular day, b) Simple bilinear interpolation of (a) to ERA5-land resolution, c) Quantile correction of (b) by mapping the modelled ECDF (from CMIP6) and the reference ECDF (from ERA5-land) for each grid point of the ERA5-land reanalysis, taking all days of the common period. 17

Figure 5: Examples of smooth (a and b) or exponential (c and d) distributions, plotted in linear (a and c) or logarithmic (b and d) scales. 18

Figure 6: Examples of transfer function between Historical Experiment values and the bias-correction increment or factor obtained from the comparison of quantile mapping (ERA5 versus Historical experiment): a) Maximum temperature, b) Maximum relative humidity; c) Precipitation. 19

Figure 7: Modelling Domains: D01 refers to the outermost domain and d02 to the nested domain (region of Greece). 21

Figure 8: Validation of the average values of the CMIP6 multi-model. Spatial distribution of the (multi-model)-(reanalysis) BIAS for the historical simulation of daily maximum temperature. Multi-model representative is chosen by using the median value in each grid point, and the climate average is compared to that obtained with ERA5-Land. 24

Figure 9: Validation of the annual cycle of the downscaled CMIP6 models: Monthly climograph for daily maximum temperature simulated by the multi-model ensemble (colour lines) for the Historical experiment, and comparison with the reference climograph simulated by the ERA5-Land. 25

Figure 10: BIAS of TMax per model, calculated month by month over the spatial average of the entire grid in the historical period (each boxplot is the 12 months). 26

Figure 11: Time series validation of Maximum Temperature for the case of study DA-01-IT (Sardinia, Italy) . Comparison between values obtained from the grids of 9km x 9km and 1km x 1km for the three scenarios: Lower, Medium and Upper. 29

Figure 12: Time series validation of Precipitation for the case of study DA-01-IT (Sardinia, Italy) . Comparison between values obtained from the grids of 9km x 9km and 1km x 1km for the three scenarios: Lower, Medium and Upper. 30

Figure 13: Example of statistical downscaling result for DA-01-IT (Sardinia, Italy), for maximum temperature values (2021-2050 average) and change values of 2071-2100 compared to 2021-2050 period, before and after the second downscaling: 9km x 9km absolute values (upper left), 9km x 9km change values (upper right), 1km x 1km absolute values (bottom left), 1km x 1km change values (bottom right). 31

Copyright © FirEURisk Consortium. All rights reserved.

Figure 14: Example of statistical downscaling result for DA-01-IT (Sardinia, Italy), for precipitation values (2021-2050 average) and change values of 2071-2100 compared to 2021-2050 period, before and after the second downscaling: 9km x 9km absolute values (upper left), 9km x 9km change values (upper right), 1km x 1km absolute values (bottom left), 1km x 1km change values (bottom right). 32

Figure 15. Maximum temperature's values of 20-years return period (left), 50-years return period (centre) and 100-years return period (right) for the historical period 1980-2004 in the DA and PS. 33

Figure 16. Wind speed's values of 20-years return period (left), 50-years return period (centre) and 100-years (right) return period for the historical period 1980-2004 in the DA and PS. 33

Figure 17. SPI6's values of 20-years return period (left), 50-years return period (centre) and 100-years (right) return period for the historical period 1980-2004 in the DA and PS. 34

Figure 18. Relative humidity's values of 20-years return period (left), 50-years return period (centre) and 100-year (right) return period for the historical period 1980-2004 in the DA and PS. 34

Figure 19. Maximum Temperature's values of 20-years return period (upper left), 50-years return period (upper right) and 100-years return period (below) for the near and far future period under RCP4.5 and RCP8.5 in the DA and PS. 39

Figure 20. Wind speed's values of 20-years return period (upper left), 50-years return period (upper right) and 100-years return period (below) for the near and far future period under RCP4.5 and RCP8.5 in the DA and PS. 40

Figure 21. SPI6's values of 20-years return period (upper left), 50-years return period (upper right) and 100-years return period (below) for the near and far future period under RCP4.5 and RCP8.5 in the DA and PS. 41

Figure 22. Relative humidity's values of 20-years return period (upper left), 50-years return period (upper right) and 100-years return period (below) for the near and far future period under RCP4.5 and RCP8.5 in the DA and PS. 42

Figure 23. Probability of exceeding a threshold for maximum temperature>35°C (upper left), wind speed>8m/s (upper right), SPI6<-1 (bottom left) and relative humidity<30% (bottom right) for the far and future periods under RCP4.5 and RCP8.5. 43

Copyright © FirEURisk Consortium. All rights reserved.

List of tables

Table 1: List of Acronyms 9

Table 2. Variables and their main characteristics selected from ERA5-Land. 12

Table 3. Information about the ten climate models belonged to the CMIP6 corresponding to the sixth report of the IPCC. Models were supplied by the Program for Climate Model Diagnosis and Intercomparison (PCMDI) archives. 16

Table 4. Daily variables generated by statistical downscaling and the specific procedures (if case). 19

Table 5: Configuration of the WRF physics parameterizations schemes used during the simulations. 22

Table 6. Selection of model and scenario to calculate future Lower, Medium and Upper scenarios for the DA-01-IT case of study. 27

Table 7. Selection of model and scenario to calculate future Lower, Medium and Upper scenarios for the whole 9km x 9km European grid. 44

Table 8. Selection of model and scenario to calculate future Lower, Medium and Upper scenarios for each case of study. 44

Copyright © FirEURisk Consortium. All rights reserved.

List of Acronyms

Table 1: List of Acronyms

List of Acronyms	
CMIP6	Coupled Model Intercomparison Project Phase 6
DA	Demonstration Area
DC	Drought Code
PS	Pilot Site
SSP	Shared Socioeconomic Pathway

Copyright © FirEURisk Consortium. All rights reserved.

1 Introduction

1.1 Purpose

This deliverable reports the methods and results of the Task 3.1.1 - "Climate change scenario data". Particularly, the main objective of this work was to provide climate projections of the variables that most influence fire risk with a 1km resolution grid in each study area. Moreover, a contrast experiment was designed by National Centre for Scientific Research Demokritos (NCSRD) to analyse the robustness of the projections.

1.2 State of the art

The probability, spread and evolution of wildfires depend to a large extent on the climatic and meteorological conditions in a given area. One of the main obstacles when studying the role of climate change in the occurrence of wildfires is that climate models have a grid with a very low resolution that is not able to capture local phenomena, and these local phenomena play a very important role in the development of wildfires. For all these reasons, it is essential that future climate projections take into account the peculiarities of each area in order to be able to study future fire risk more reliably. To provide adequate climate information at a local scale, it is necessary to apply some kind of downscaling process based on statistical or dynamical approaches (Ribalaygua et al. 2013, Monjo et al. 2016). For instance, dynamical downscaling of CMIP6 is currently running (Euro-CORDEX 2022), while statistical downscaling efforts were recently performed in the Chelsa project (Brun et al. 2022) and Copernicus-C3S (2020, 2022).

Fire danger conditions are influenced by 2m maximum temperature (TX), relative humidity (RH), and wind speed at 10 m (WS), parameters that were documented in the official wildfire database immediately after every fire event, according to Mitsopoulos et al. (2017). We also used the Standardised Precipitation Index (SPI) which characterises meteorological droughts for a certain period. The SPI is calculated by fitting a probability density function ('gamma') to a given frequency distribution of historical precipitation and then the probabilities are transformed into a normalised distribution with a mean equal to zero and a variance of one, developed by Mckee et al. (1993). More specifically, as suggested by Bifulco et al. (2014), the medium-term drought index (SPI6) in September provided the best explanation for burned areas because it identifies specific periods where the shortage of water is crucial to increase wildfire extent. Additionally, Wu et al. (2007) and Karavitis et al. (2014) point out in their studies that semi-arid and arid areas could give an unreliable estimation of meteorological indices computed at short accumulation periods (e.g., 3-months). Moreover, Dimitrakopoulos et al 2011 found that the majority of fires occur during the month of September for the Eastern Mediterranean environment as no rain has occurred since late spring and consequently creating a prolonged drought period (Rovithakis et al. 2022).

1.3 Structure of the report

The report is structured in three main sections: (2) ***Study area and data***, to define the framework area and data used to provide climate projections in two spatial scales (Europea and demonstration areas); (3) ***Methodology,*** to describe the main details on the approaches used in the climate simulations at different spatial resolutions and under several models and scenarios; (4) ***Results, products and validation***, to present the validation results and the final products to be used.

Copyright © FirEUrisk Consortium. All rights reserved.

2 Study area and data

2.1 Study area: Demonstration Areas (DA) and Pilot Sites (PS)

The Study area of FirEURisk is Europe, with borders {32°N, 72°N; 15°W, 35°E}. Most of the Pilot Sites and Demonstration Areas are located along the Mediterranean Basin, covering extensive areas within Croatia, France, Greece, Italy, Portugal and Spain. In addition, there are other areas of study located in Czech Republic, Germany, Poland, Romania, Sweden, Ukraine and the United Kingdom (Figure 1).

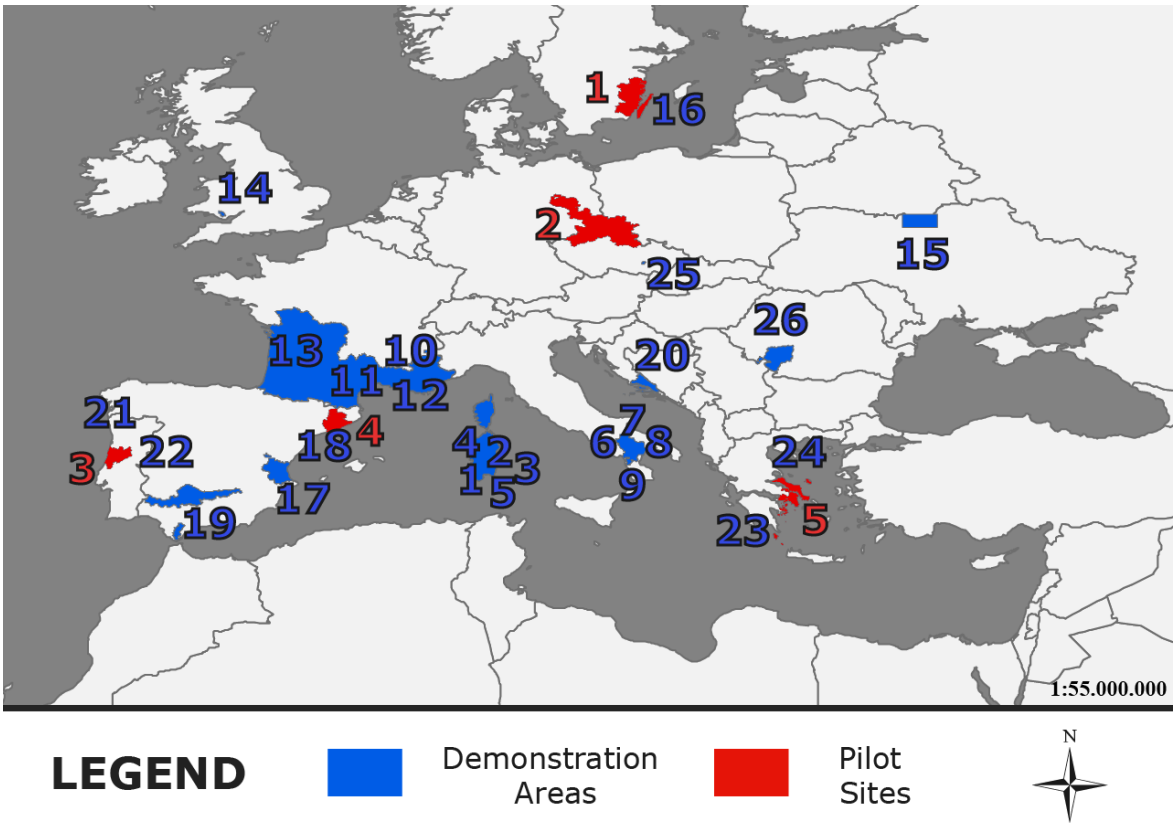


***Figure 1**: Study area of FirEURisk, with borders in {32°N, 72°N; 15°W, 35°E} and location of the Demonstration Areas and Pilot Sites.*

Copyright © FirEURisk Consortium. All rights reserved.

2.2 Atmospheric reanalysis: ERA5-Land

European ERA5 (atmospheric) and ERA5-Land (surface) reanalyses are selected for the task T3.1.1, for several reasons: 1) they are developed by the European Centre for Medium-Range Weather Forecasts (ECMWF), whose main geographical area of work is where FirEUrisk takes place, and whose weather forecasts are proved to be among the best available; 2) They are the most current versions of the European reanalysis which entails an improvement in spatial and temporal resolution with respect to the previous ones; and 3) their download is free of charge through the Copernicus program (Climate Change Service: DOI: 10.24381/cds.adbb2d47). The ERA5/ERA5-Land were released in 2019 and their temporal coverage is still being expanded. ERA5-Land is the version for surface variables, and it only covers land terrain, but worldwide with fine resolution, providing data for up to 50 different variables.

The **FirEUrisk grid is based on the ERA5-Land**, which provides 196367 inland points. ERA5-Land's coverage is a global grid with a spatial resolution of 0.073º x 0.073º (approx. 9km x 9km). Its vertical coverage ranges from 2 metres above the surface level to a soil depth of 289 cm and 4 levels of the ECMWF surface model: Layer 1: 0-7cm, Layer 2: 7-28cm, Layer 3: 28-100cm, Layer 4: 100-289cm. Some parameters are defined at 2 m over the surface. ERA5-Land gives hourly data from January 1981 to present (data are updated monthly with a delay of about three months relative to the actual date).

From all the variables available to download, only some of them were firstly identified to be used; mostly those related to the usual atmospheric observations needed from weather stations: 2m Air Temperature, Humidity, Total Precipitation, U Component of the Wind, V Component of the Wind (Table 2).

***Table 2**. Variables and their main characteristics selected from ERA5-Land.*

Variable	Daily scale	Monthly scale	Comments
Hourly temperature	-Maximum temperature -Minimum temperature -Mean temperature	-Absolute maximum temperature -Mean maximum temperature -Absolute minimum temperature -Mean minimum temperature -Mean temperature	Hourly temperature values allow us to obtain with great detail not only maximum and minimum daily temperature but also to obtain mean daily temperature with more significance than when obtained only with max and min values.
Hourly dew point temperature	-Maximum specific temperature -Maximum relative humidity -Maximum Heat Index	-Maximum specific temperature -Maximum relative humidity -Maximum Heat Index	Dew point Temperature is a variable that points at which temperature value the atmosphere would reach saturation and its moisture would start condensing in droplets. Therefore, it is an indicator of the net content of moisture of the atmosphere, being useful to get the Specific Humidity (q); moreover, the closer this value is to the actual temperature, the higher that Relative Humidity (RH) will be. Thus, Dew point Temperature at this hourly scale gives us great information about the moisture content of the atmosphere in each hour of the day, and allow us, by crossing these values with those hourly and daily values of temperature previously obtained, to obtain several derived variables, such as: Maximum q, maximum HR or Heat Index.

Copyright © FirEURisk Consortium. All rights reserved.

Hourly precipitation	24-h accumulation of precipitation	-Maximum 24-h accumulation of precipitation of the month -Monthly accumulation of precipitation	Precipitation hourly values have been aggregated at daily intervals to obtain the 24-h accumulation of precipitation for each day. Daily values are afterward treated to obtain at monthly scale both monthly total precipitation for each point and the maximum precipitation accumulated at 24h for each month. Precipitation units were adapted from "m" to "mm" for a more intuitive use.
Hourly wind (U and V components)	Maximum daily mean wind	Maximum daily mean wind	In the case of wind, ERA5-Land available hourly data corresponds to both U and V wind components with the hourly mean values. Both components have been composed at hourly intervals according to the following rule: Wind $=\sqrt{(U^2 + V^2)}$ since U and V are vectorial components of the wind module. With this procedure, we have obtained the mean hourly wind, which allows us to calculate its maximum values for each day and month.
Solar radiation	Solar radiation	Average solar radiation	Total solar radiation of ERA5-Land

The ERA5 is the last atmospheric reanalysis released from the ECMWF. Available since July 2019, it is the most accurate reanalysis available so far. It works with a huge set of data and observations from weather stations, soundings, satellites and other different reanalysis (like oceanic) as input at different atmospheric and sea levels. This way, ERA5 tries to reproduce with the most accuracy the real values that defined the atmospheric situation at a given time of the past. Due to its requirements of high-quality input, only data after satellite release is available.

ERA5 covers all of Europe's land territory with a regular spatial resolution of 0.25° (30 km approx.). The monthly available variables are precipitation, mean temperature, runoff (total, surface and sub-surface), and SST for the period 1979 to present.

The files present NetCDF format (ERA5_variable_monthlyEU.nc), with one file for each variable, since the monthly basis resolution allows incorporating the whole-time coverage in it. As long as ERA5 data is available, we strongly encourage its use over CRU data, in addition to being the only source of Runoff available (see more information regarding the dataset in https://cds.climate.copernicus.eu/cdsapp#!/dataset/reanalysis-era5-single-levels?tab=overview).

Copyright © FirEURisk Consortium. All rights reserved.

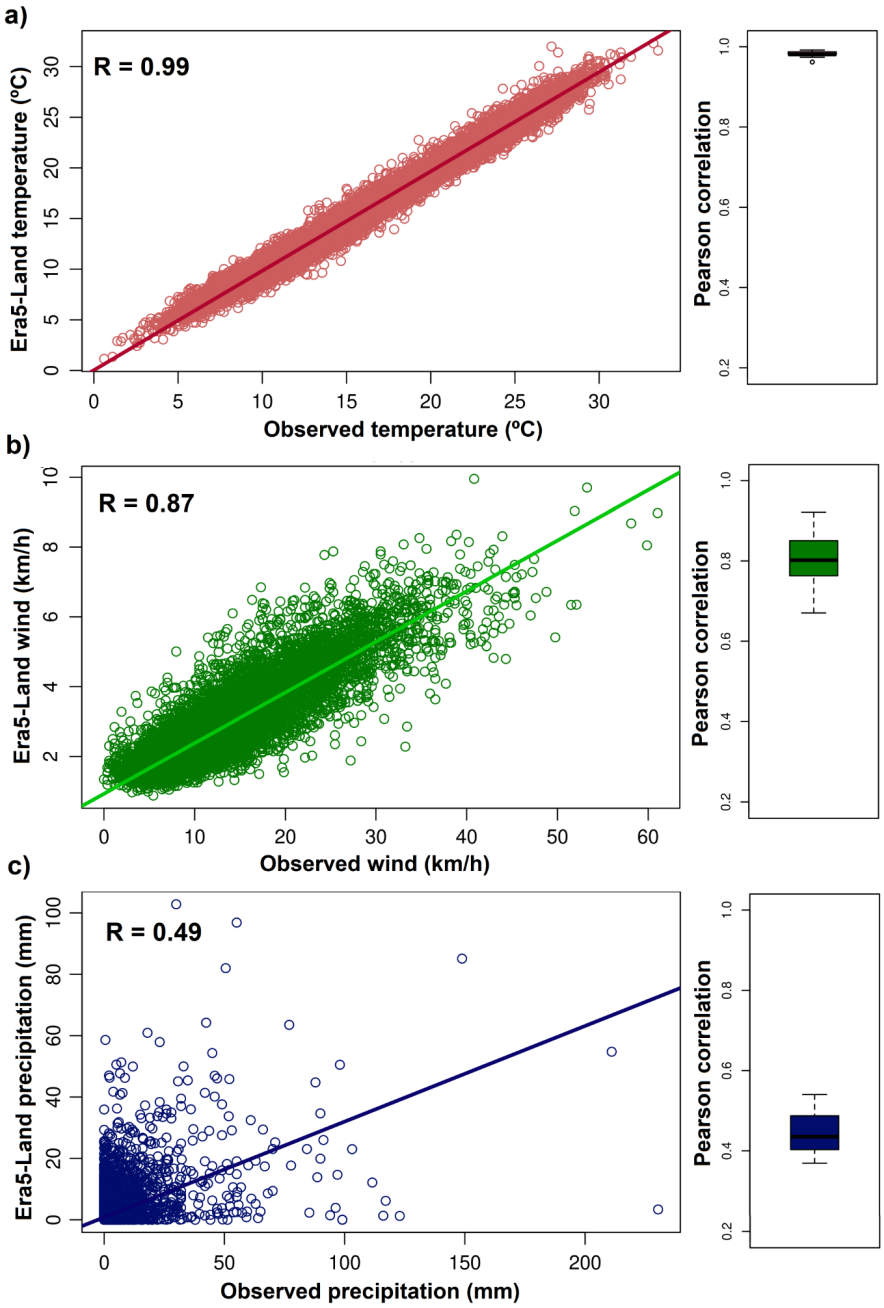


Figure 2: *Validation of the daily surface fields simulated by ERA5-Land: Pearson correlation between observations and simulations for (a) maximum temperature, (b) mean wind and (c) total precipitation for Valencia (left) and for a set of ten reference observatories in Europe (right).*

Copyright © FirEURisk Consortium. All rights reserved.

2.3 Earth System Models: CMIP5 and CMIP6 experiments

For the Task 3.1.1, we use 10 climate models on a daily resolution, collected from the Coupled Model Intercomparison Project (CMIP) - Phase 6 (CMIP6). CMIP is a collaborative framework designed to improve knowledge of climate change. It was organised in 1995 by the Working Group on Coupled Modelling (WGCM) of the World Climate Research Programme's (WCRP). Throughout the different phases that this project has gone through, improvements have been introduced in the quality of the climate models up to the current Earth System Models (ESM). Likewise, new emission scenarios have been defined in each of the phases, adjusting to the new needs for adaptation and mitigation in the face of climate change.

The structure of the CMIP6 has been extended with respect to CMIP5 by providing an equivalent framework named CMIP Diagnostic, Evaluation and Characterization of Klima (DECK), together with a set of Endorsed MIPs to improve the description of aspects of climate models beyond the core set of common experiments included in DECK (https://www.wcrp-climate.org/wgcm-cmip/wgcm-cmip6)

CMIP6 has a common set of future scenarios comprising land use and emissions as required for the future Shared Socio-Economic Pathways (SSPs). New scenarios span a similar range as the RCPs, but fill critical gaps, including: Role of specific forcings, such as land use and short-lived species (air quality), the effect of a peak and decline in forcing and the consequences of scenarios that limit warming to below 2 °C (Eyring et al., 2016)

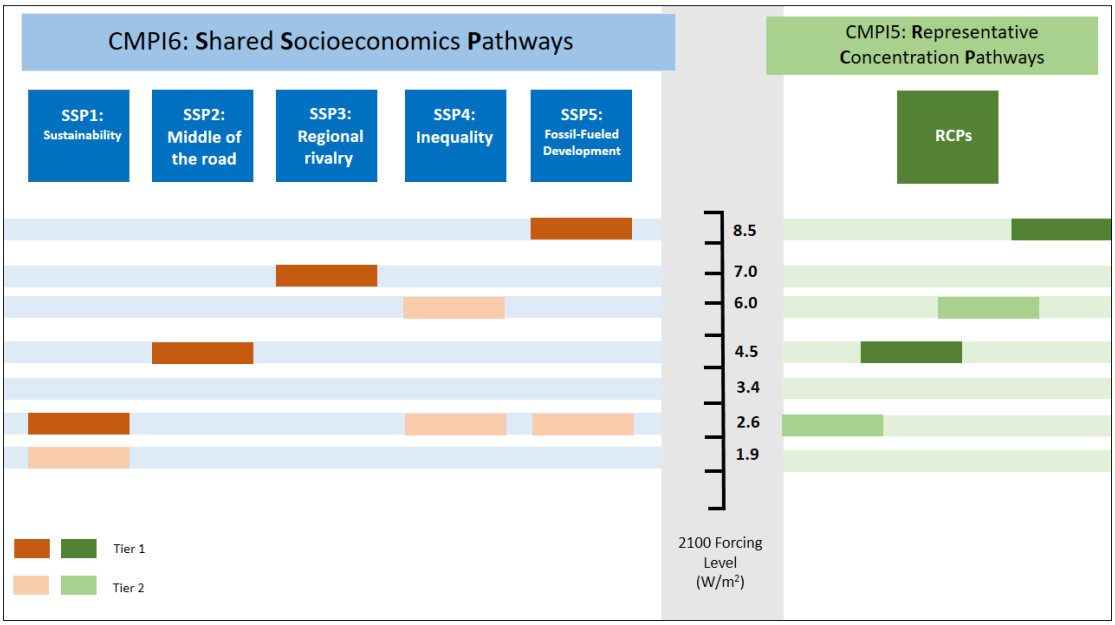


***Figure 3**: Comparison between the scenarios defined under CMIP6 and those defined under CMIP5. Tier 1 and Tier 2 are defined as those scenarios which are to be provided on an obligatory and optional basis, respectively, by all the climate models which form part of each phase of the CMPI.*

Copyright © FirEURisk Consortium. All rights reserved.

Shared Socioeconomic Pathways (SSPs) are scenarios of projected socioeconomic global changes up to 2100 describing alternative socio-economic developments (**Figure 2**).
Each model provides a historical experiment, from 01/01/1950 to 31/12/2014 and 4 future scenarios (ssp126, ssp245, ssp370 and ssp585) ranging from 01/01/2015 to 31/12/2100. The relation of the selected models is detailed in Table 3:

***Table 3**. Information about the ten climate models belonged to the CMIP6 corresponding to the sixth report of the IPCC. Models were supplied by the Program for Climate Model Diagnosis and Intercomparison (PCMDI) archives.*

CMIP6 MODELS	Resolution	Responsible Centre	References
BCC-CSM2-MR	1,125º x 1,121º	Beijing Climate Centre (BCC), China Meteorological Administration, China.	Wu, T. et al. (2019)
CanESM5	2,812º x 2,790º	Canadian Centre for Climate Modelling and Analysis (CC-CMA), Canadá.	Swart, N.C. et al. (2019)
CNRM-ESM2-1	1,406º x 1,401º	CNRM (Centre National de Recherches Meteorologiques), Meteo-France, Francia.	Seferian, R. (2019)
EC-EARTH3	0,703º x 0,702º	EC-EARTH Consortium	EC-Earth Consortium. (2019)
GFDL-ESM4	1,250º x 1,000º	National Oceanic and Atmospheric Administration (NOAA), E.E.U.U.	Krasting, J.P. et al. (2018)
MPI-ESM1-2-HR	0,938º x 0,935º	Max-Planck Institute for Meteorology (MPI-M), Germany.	Von Storch, J. et al. (2017)
MRI-ESM2-0	1,125º x 1,121º	Meteorological Research Institute (MRI), Japan.	Yukimoto, S. et al. (2019)
UKESM1-0-LL	1,875º x 1,250º	Uk Met Office, Hadley Centre, United Kingdom	Good, P. et al. (2019)
NorESM2-MM	1,250º x 0,942º	Norwegian Climate Centre (NCC), Norway.	Bentsen, M. et al. (2019)
ACCESS-ESM1-5	1,875º x 1,250º	Australian Community Climate and Earth System Simulator (ACCESS), Australia	Ziehn, T. et al. (2019)

A grid covering Europe, between latitudes 32°N and 72°N and longitudes between 15°W and 35°E, has been chosen for the study. The surface variables available from CMIP6 are wind, temperature, humidity and rainfall at a daily timescale. Other variables related to geopotential fields (e.g. 1000, 850, 500 and 300hPa) are also available too.

Moreover, as a control experiment, CMIP5 EC-Earth (EC-EARTH Consortium, 2017) was used to compare with CMIP6 multi-model performance for two specific study areas corresponding to MED-Greece (PS-05 and DA-23).

Copyright © FirEURisk Consortium. All rights reserved.

3 Methodology

3.1 CMIP6 downscaling to 0.073°×0.073° resolution grid

The selection of the downscaled method can be a dynamical or statistical approach (Ribalaygua et al. 2013). In the beginning of the project, dynamical downscaling of CMIP6 projections was not available yet for Europe (Euro-CORDEX 2022), while previous statistically downscaled products did not provide daily resolution for the climate projections (e.g. Chelsa project, Brun et al. 2022) or were performed after the FirEURisk products (e.g. Copernicus-C3S 2022).

In FirEURisk, climate projections were obtained by using a downscaling approach of transfer functions, based on parametric quantile-quantile mapping (Benestad 2010; Monjo et al. 2014) by using ERA5-Land as a reference (about 9km of spatial resolution). A two-step method was commonly applied to all the variables and projections (10 climate models x 4 SSPs, when available):

- Given a specific historical experiment, each (daily) climate variable is downscaled to each (reference) grid point of the ERA5-Land, by comparing the Empirical Cumulative Distribution Function (ECDF) of the reanalysis and the ECDF of the historical experiment of the climate model, previously bilinearly interpolated (**Figure 4**). From this comparison, a quantile-quantile mapping is obtained and used to fit parametric functions. In our case, the selected functions are polynomial curves to reduce the computational cost compared to exponential distributions of Monjo et al. (2014, 2016).
- Finally, parametric functions are applied to correct the SSP projections on a daily scale. These downscaled projections have been obtained for a grid covering all European countries, with the same spatial resolution as the ERA5-Land.

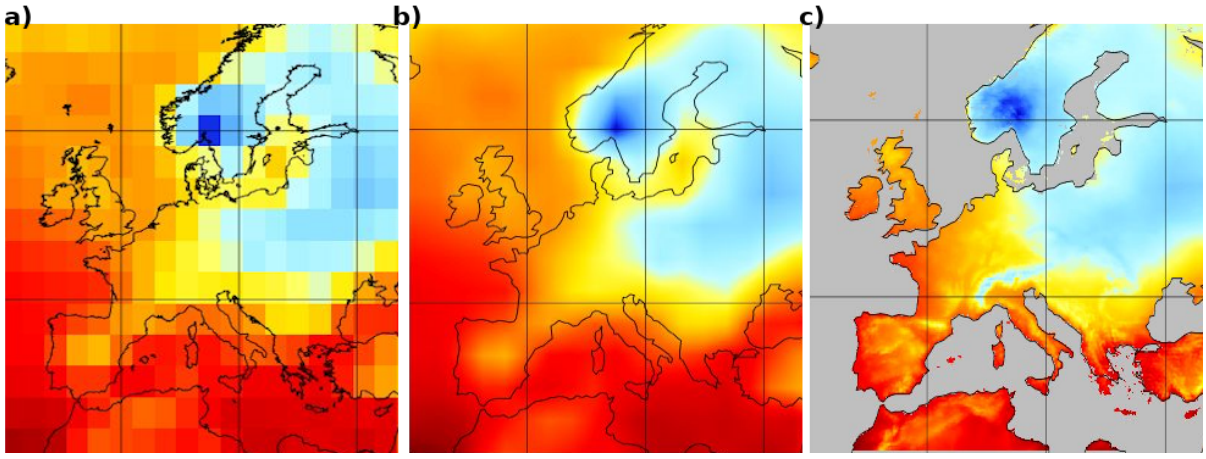


Figure 4: *Example downscaling processes of a daily field output from CMIP6 Earth System Models, applying transfer functions: a) Original gridded model output of a particular day, b) Simple bilinear interpolation of (a) to ERA5-land resolution, c) Quantile correction of (b) by mapping the modelled ECDF (from CMIP6) and the reference ECDF (from ERA5-land) for each grid point of the ERA5-land reanalysis, taking all days of the common period.*

Depending on whether the climate variable is more similar to (*f*) **smooth** (linear uniform, Gaussian) **distributions** (e.g. temperature, humidity) or more similar to (*g*) **exponential** (log-normal, Weibull, gamma,...) **distributions** (Figure 3),

Copyright © FirEURisk Consortium. All rights reserved.

the transfer functions (polygonal curves) are fitted from (*f*) **increments** or (*g*) **factors** obtained by comparison of each target quantile value (from HIST) and the corresponding reference quantile value (from ERA5). That is:

$$f := mapping(sort(ERA5),\ sort(ERA5) - sort(HIST))$$
$$g := mapping(sort(ERA5),\ sort(ERA5)/sort(HIST)) \quad for\ ERA5 > 0\ and\ HIST > 0$$

MOD_smooth_var = MOD_smooth_var + *f*(MOD_smooth_var)
MOD_exponential_var = MOD_exponential_var * g(MOD_smooth_var)

That means that extreme values (when MOD is outside the distribution tails of HIST) are transformed with the same increment (*f*) or factor (*g*) than the empirical tails of the training sample (HIST). This method can be directly applied for classical scalar variables (temperature, precipitation, humidity, pressure, ...), with smooth or exponential distributions, according to up 6th degree polynomial fits applied to linear or logarithmic factors (**Figure 4**). As climate change will produce values located outside the historical tails, these values are corrected with the **last truncated factor** of the tailed mapping (f or g).

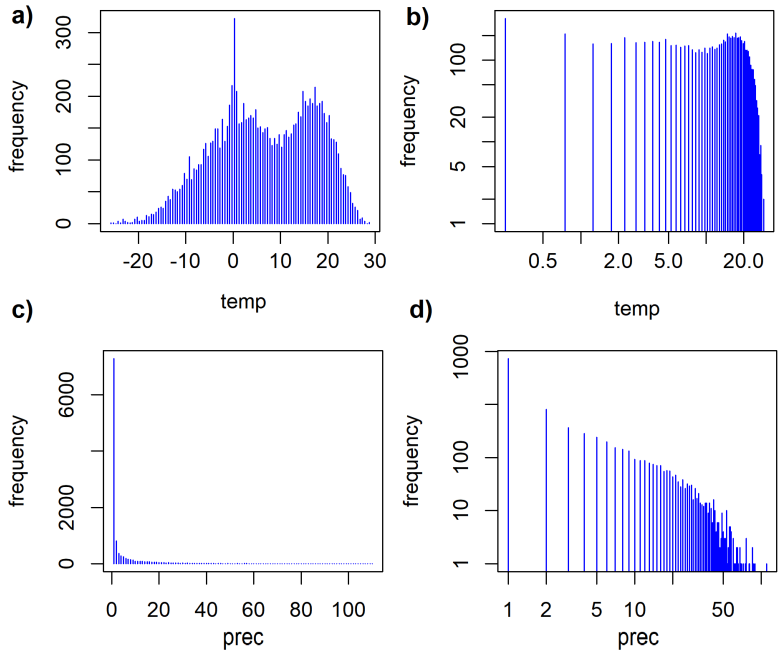


Figure 5: *Examples of smooth (a and b) or exponential (c and d) distributions, plotted in linear (a and c) or logarithmic (b and d) scales.*

Copyright © FirEURisk Consortium. All rights reserved.

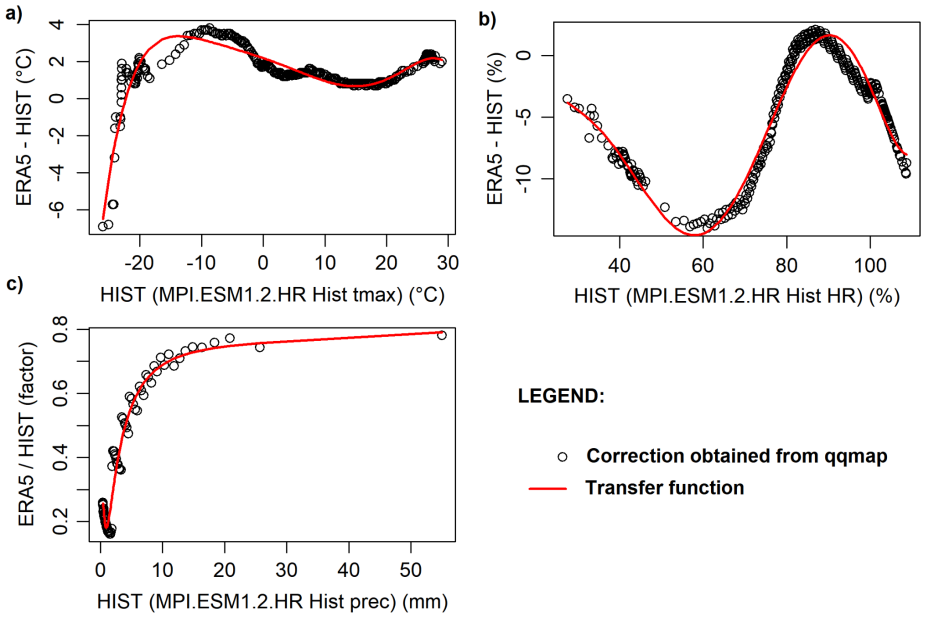


Figure 6: *Examples of transfer function between Historical Experiment values and the bias-correction increment or factor obtained from the comparison of quantile mapping (ERA5 versus Historical experiment): a) Maximum temperature, b) Maximum relative humidity; c) Precipitation.*

However, some variables require special attention. This is the case of vectorial variables (e.g. wind), derived variables (potential evapotranspiration) or flux variables (short- and long-wave down radiation). For these variables, additional procedures were performed (Table 4)

Table 4*. Daily variables generated by statistical downscaling and the specific procedures (if case).*

Variable	Type	Specific procedures
2m air temperature (°C)	**TMax** - Maximum temperature **TMin** - Minimum temperature **TMean**-Mean temperature	It is directly corrected by parametric quantile mapping (smooth distribution). Diurnal range is defined as TMax - TMin Mean temperature is defined as TMean = (TMax + TMin)/2
2m air humidity (%)	**HRMax** - Maximum relative humidity **HRMin**- Minimum relative humidity	It is directly corrected by parametric quantile mapping (smooth distribution). A post-process is considered for saturing the values lower than 0% and higher than 100%
surface precipitation (mm)	**tpr** - Total daily (24-h) precipitation	It is directly corrected by parametric quantile mapping (exponential distribution).

Copyright © FirEURisk Consortium. All rights reserved.

10m Wind (m/s)	**WM**- Mean wind (Module, direction, **U, V** - Components	Wind module $W = \sqrt{(U^2 + V^2)}$ is directly corrected (W') like an exponential variable. Since U and V are not totally independent components (because some directions linked to topography can be more frequent than others), it is necessary to separate two contributions: - Mutual dependent contribution <U> = F(<V>) - Residual contributions, [U] := U - <U> and [V] := V - <V> Therefore, three variables are corrected as smooth distributions: [U], [V] and <X> (only <U> or <V>), then obtaining V' = [V]' + <V> and U' = [U]+F(<V>'). Finally, U' and V' are normalised to obtain direction ***α***, and final values are U'' = W'cos***α*** and are V'' = W'sin***α***
Solar radiation (W·m-2)	**LWD**- Long-wave down radiation **SWD**- Short-wave down radiation	It is corrected from total "solar radiation" of ERA5-Land and then long- and short-wave radiation are split according to the original rate of the model.

3.2 CMIP6 downscaling to 1km x 1km resolution grid

To achieve this, a *topography-based transfer function was* applied to the 9km-resolution downscaled model outputs, trained with the time series from the ERA5-Land reanalyses. Particularly, for each climate variable simulated by the CMIP6 models, the statistical downscaling was applied according to three steps:

1) For all the variables and for each projected day (with 0.073°×0.073° resolution), a purely geo-statistical was performed to a 1km×1km grid by using AIC-based stepwise regression with topological and geographical parameters **(altitude, latitude, longitude and distance to the Atlantic Ocean and Mediterranean Sea**), and bilinear model for the residual errors.
2) Similarly, for each targeted day, residual errors of the AIC-based stepwise regression were interpolated from the original grid (0.073°×0.073°) to the final 1km×1km grid by using a bilineal model.
3) Finally, the projected value for each day is obtained by adding the result of Step (1) and Step (2), obtaining climate scenarios in a 1km×1km grid at a daily timescale.

3.3 CMIP5 contrast experiment in MED-Greece

3.3.1 Motivation of a contrast experiment

Dynamical downscaling has a large computational cost in comparison with the statistical downscaling and therefore, it is not possible to apply to all the regions and all the climate models. In order to test and check the robustness of the results, a *contrast experiment* was designed by NCSRD for the MED-Greece demonstration. In this case, CMIP5 climate projections of EC-Earth were dynamically downscaled by using the *Weather Research and Forecasting Model* (WRF) at a resolution of 5 km x 5km. The Representative Concentration Pathways (RCP) used were the core scenarios RCP4.5 and RCP8.5. In this way, we can compare two very different approaches:

- Statistically downscaled CMIP6 multi-model SSP projections

Copyright © FirEURisk Consortium. All rights reserved.

- Dynamical downscaled CMIP5 EC-Earth-WRF RCP projections

Secondly, we have proceeded with extreme value analysis according to Task 3.1. The analysis involved, under the 2 RCPs scenarios and two different future periods, the estimation of climate values (maximum temperature, wind speed and 6-months Standardised Precipitation Index -SPI- of September) for various return periods (20, 50, 100 years) and the probability of exceeding a value which favour fire events, based on extreme value theory for the selected pilot and demonstration areas in Greece. Finally, a WRF model climate data scenario of extreme fire event(s) has been prepared on the basis of these thresholds of climate variables.

3.3.2 Description of the experiment

EC-Earth model (Hazeleger et al. 2010) is a full physics seamless atmosphere–ocean sea- ice coupled earth system prediction model and developed from the operational Integrated Forecast System (IFS) cycle 31r of ECMWF. The set-up of the atmospheric model in the EC-Earth version 2.3 corresponds to the use of a horizontal spectral resolution of T159 (triangular truncation at wavenumber 159), roughly 125 km, and a vertical grid with vertical 62 levels of a terrain-following mixed sigma-pressure hybrid coordinates, of which about 15 are within the planetary boundary layer (PBL). EC-Earth model demonstrates very good forecasting skill and can also be used for climate studies, supporting emerging seamless prediction strategies. In addition, the model simulates well the tropospheric fields and the dynamic variables, but not as well the surface temperature and fluxes (Hazelger et al 2012). ECEarth2 has been used for simulations under CMIP5 and in a range of climate studies, (e.g. Koenigk et al. 2013, Seneviratne et al. 2013)
We performed regional climate simulations for the area of Greece with the non-hydrostatic Weather Research and Forecasting model (WRF/ARW, v3.6.1) (Skamarock et al. 2008) with two domains. The first domain (d01) of 20 km resolution was centred in the Mediterranean basin at 42.5 N and 16.00E, and a second nested domain of 5 km over Greece (d02).



Figure 7. *Modelling Domains: D01 refers to the outermost domain and d02 to the nested domain (region of Greece).*

Copyright © FirEURisk Consortium. All rights reserved.

Both domains have 40 vertical layers. The model domains share the same options of physics parameterizations. The boundary conditions for the climate change assessment derived from EC-EARTH climate simulations for RCP4.5 and RCP8.5 scenario and encompassed time slices representative of the historical (1980–2004), midcentury (2025–2049), and end of century (2075–2099) periods. For the future projections, the equivalent-CO2 concentration was updated every year according to the emission scenario in the WRF simulations. The model setup was extensively analysed in the study of Politi et al. (2021) which has proved the value of high-resolution dynamical downscaling, for the historical period for the area in Greece that yielded more realistic topographical-induced precipitation and temperature fields with their extremes compared to reanalysis dataset. The physics parameterizations are summarised in table 2. Moreover, model results were also validated with observed data for mean seasonal daily Global Horizontal Irradiation (GHI), clear-sky fraction/days (Katopodis et al. 2020) and wind speed at 10m (Katopodis et al. 2021).

Table 5: Configuration of the WRF physics parameterizations schemes used during the simulations.

Physics schemes		
PBL scheme	Mellor–Yamada–Janjic scheme (MYJ)	Mellor and Yamada 1982
Cloud microphysics scheme	WRF single-moment six-class scheme (WSM-6)	Hong and Lim 2006
Cumulus scheme	Betts–Miller–Janjić (BMJ)	Janjić 2001
Land surface model scheme	Noah LSM	
longwave and shortwave radiation scheme	Rapid Radiative Transfer Model (RRTMG)	Iacono et al. 2008

Thus, WRF will provide the following climate data in daily temporal resolution for MED-Greece at 5 km resolution:

Climate variables
Maximum temperature
Minimum temperature
Precipitation
Relative humidity
Wind speed

These datasets can be used as input to develop a methodology for specific extreme fire events or models. The methodology of data processing refers to the definition and recognition of risk parameters as return periods, based on the Extreme Value Analysis (EVA), for the specific case study in order to evaluate the intensity and frequency of rare fire events that lie far in the tails of the probability distribution of weather variables. The processing was implemented through R-markdown scripts and the extreme value theory is applied through extRemes package (Gilleland et al 2016). *Extreme Value Theory* is a well established approach for the determination of risk associated with the occurrence of climate extremes that lie far in the tails of the probability distribution of weather variables.

The extreme value distributions (EVD's) are generalised extreme value (GEV) or generalised Pareto (GP). Generalised Extreme Value distribution (GEV) is most used in modelling annual extremes of climate parameters for various return periods and the probability of occurrence based on thresholds. Thresholds are quantitative critical values that may be related not only with extreme phenomena (fires, extreme weather events), but to mean climate values, standard deviation of a variable etc., with significant change, depending on the problem to solve. It is possible

Copyright © FirEURisk Consortium. All rights reserved.

to account for non-stationary conditions (climate change) in extreme value analysis, but scientists are still debating the best way to do this. Nevertheless, adaptation strategies should begin to take into account the observed and projected changes in extremes.

The concept of return period is particularly useful to assess the long-term tendency of extreme values, the values of interest in hazard studies. In this case, we can fit the EVD to the tail of the simulated data and extrapolate to a range of years well beyond the number of years available in the dataset (Coles, 2001). Return levels are essentially the same as quantiles. A return level with a return period of T = 1/p years is a high threshold x(p) (e.g., annual peak flow of a river) whose probability of exceedance is p. For example, if p = 0.01, then the return period is T = 100 years.

The Generalised Extreme Value (GEV) distribution was introduced into meteorology by Jenkinson (1955) and is used extensively there to model extremes of natural phenomena such as precipitation (Gellens, 2002), temperature (Nogaj et al., 2007) and wind speed (Coles and Casson, 1999). The cumulative distribution function (CDF) of the GEV distribution is:

$$F(x;\mu,\sigma,\xi) = \begin{cases} \exp\left\{-\left[1+\dfrac{\xi(x-\mu)}{\sigma}\right]^{-\frac{1}{\xi}}\right\}, & \xi \neq 0 \\ \exp\left\{-\exp\left[-\dfrac{x-\mu}{\sigma}\right]\right\}, & \xi = 0 \end{cases}$$

Where the three parameters, “ξ” represent the shape, which characterises the heaviness of the distribution's tails, “μ” the location that determines the shift of the distribution relative to the standard GEV, and “σ” the scale which defines the spread of the distribution. The GEV is often called a family of F(x)s because it encompasses the three types of EVD’s: If the shape parameter is zero, then the F is defined by continuity and Gumbel (shape = 0, light tail), used extensively in hydrology, meteorology and engineering, Frechet (shape > 0, heavy tail) and the reverse Weibull (shape < 0, bounded upper tail at location - scale/shape).

When comparing observations and model output, it is important to know what scales are represented by the observational data sets and how they might differ from model output to avoid misinterpretation. Global climate models are not yet able to provide scenarios with sufficient detail at the regional and local scale for many applications. Their coarse spatial resolution affects in particular the projections for changes in extremes because extremes are often smaller in extent than the effective spatial resolution of the models. For this reason, downscaling (or regionalization) of global climate model projections using regional climate models (nested in the global models) or statistical techniques provides additional useful information (Giorgi, 2008). The application of this classic theory assumes that time series are stationary. Adjusted techniques are recommended when there are indications for non-stationarity.

Although very long period return values can be calculated (for example, once-in-thousand-year levels) from the fitted distribution, the confidence that can be placed in the results may be minimal if the length of the return period is substantially greater than the period covered by the sample of extremes. Estimating return levels for very long return periods is prone to large sampling errors and potentially large biases due to inexact knowledge of the shape of the tails of a distribution. Generally, confidence in a return level decreases rapidly when the period is more than about two times the length of the original data set.

Copyright © FirEUrisk Consortium. All rights reserved.

4 Results, products and validation

4.1 CMIP6 downscaling to 0.07°×0.07° resolution grid

Validation results showed that, on average, most downscaled models presented low BIAS. For instance, maximum temperature simulated by the median of the climate models is between -1 and +1ºC.

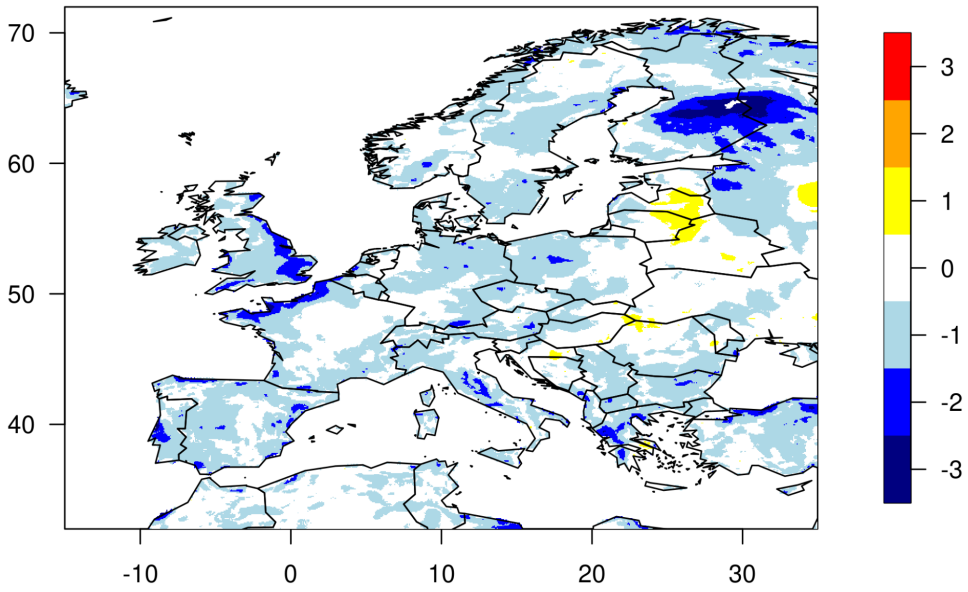


Figure 8: *Validation of the average values of the CMIP6 multi-model. Spatial distribution of the (multi-model)-(reanalysis) BIAS for the historical simulation of daily maximum temperature. Multi-model representative is chosen by using the median value in each grid point, and the climate average is compared to that obtained with ERA5-Land.*

If the monthly average value for the entire grid is taken into account, the figure shows that the climate models capture the temperature annual cycle. Results for summer and autumn months are excellent, where models practically have no error with respect to the reanalysis values. On the other hand, all the models tend to underestimate temperature in spring months and about half of them underestimate temperature in winter months.

Copyright © FirEURisk Consortium. All rights reserved.

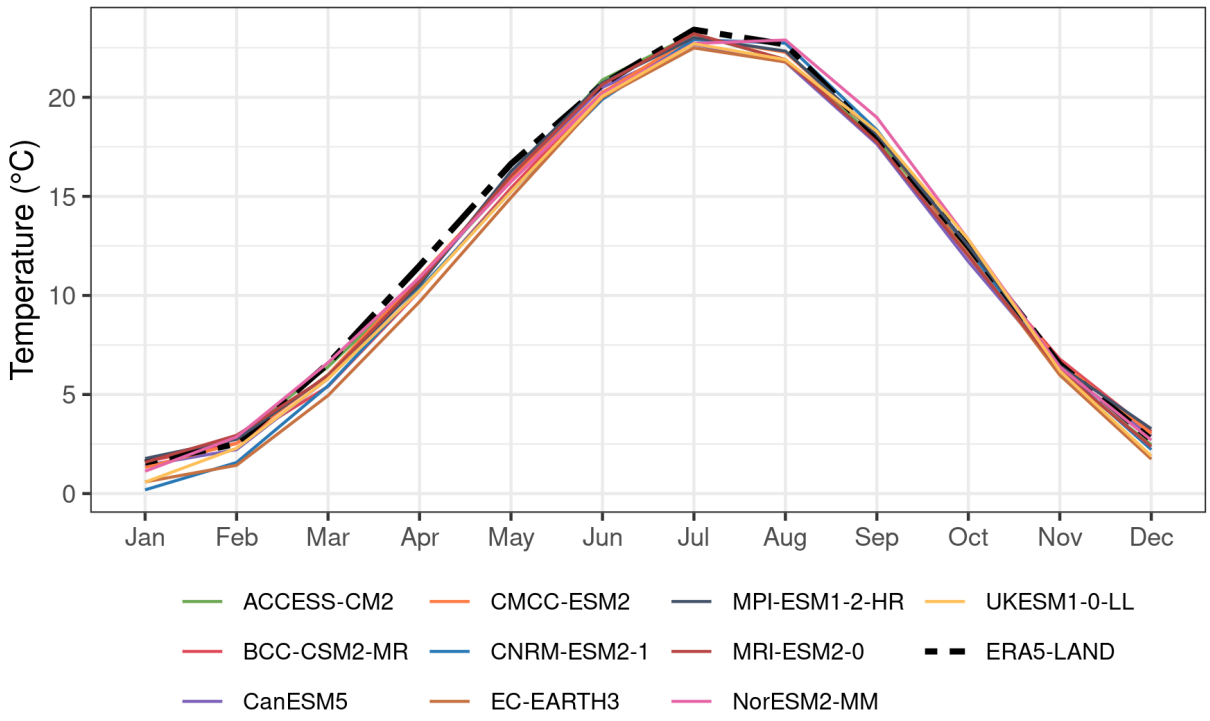


Figure 9: *Validation of the annual cycle of the downscaled CMIP6 models: Monthly climograph for daily maximum temperature simulated by the multi-model ensemble (colour lines) for the Historical experiment, and comparison with the reference climograph simulated by the ERA5-Land.*

The figure below represents, for each climate model, the monthly BIAS averaged for every cell of the grid. The main conclusion is that only two models (MPI-ESM1-2-HR and NorESM2-MM), present a BIAS whose median is around 0. The rest of them tend to underestimate temperature. Most models present median BIAS around -0.5°C and the highest BIAS do not exceed -2°C in winter months.

Copyright © FirEURisk Consortium. All rights reserved.

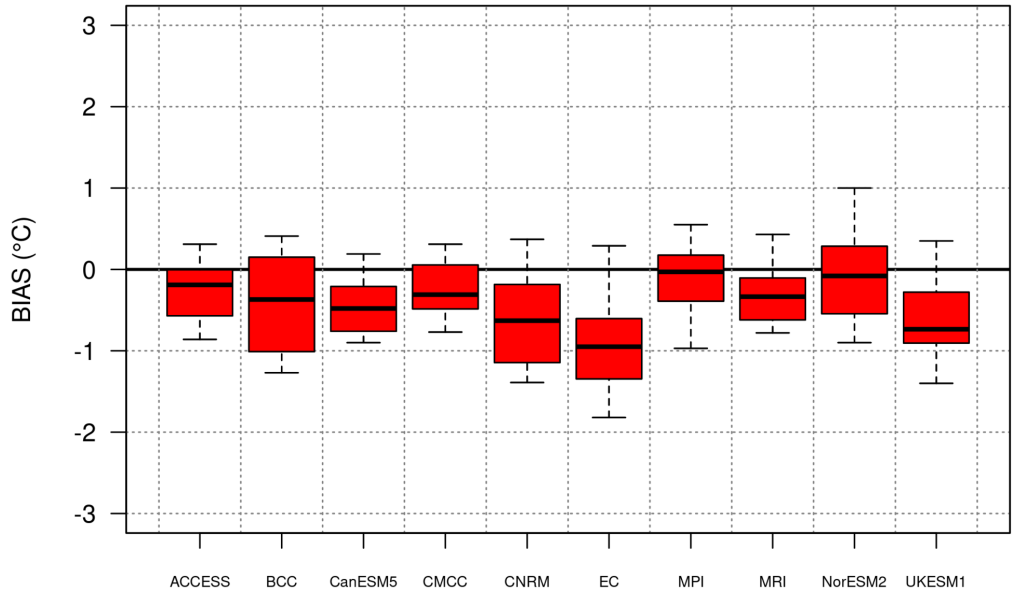


Figure 10: *BIAS of TMax per model, calculated month by month over the spatial average of the entire grid in the historical period (each boxplot is the 12 months).*

In short, the values come out well ordered for all the scenarios except for the SSP1-26 in temperature and SSP3-7.0 for precipitation.

4.2 CMIP6 downscaling to 1km x 1km resolution grid

4.2.1 Description of the experiment

For each region of study, a downscaling process has been carried out for all the climatic variables. Thus, the original European 9km x 9km resolution grid has been downscaled to a 1km x 1km resolution grid only in these areas through the methodology described in 3.2.

For each region of study, three different scenarios have been taken into account when calculating future climatic variables: lower, medium and upper. In order to calculate these scenarios, the main factor taken into consideration has been the change of the Drought Code between the periods 2015-2044 and 2071-2100. Models missing Relative Humidity (BCC-CSM2-MR, NorESM2-MM and UKESM1-0-LL) have not been considered for this calculation. For the other 7 models and its respective scenarios (ssp126, ssp245, ssp370 and ssp585) the Drought Code has been obtained for the European grid (9km x 9km) for the whole time series (2015-2100). Once the Drought Code has been obtained, it has been averaged for 30 years period (2015-2044 and 2071-2100) and the difference between the two periods has been calculated. The Drought Code differences between the two periods have been sorted and the model and scenario have been selected as follow:

Copyright © FirEURisk Consortium. All rights reserved.

- Lower scenario: Model and scenario whose DC difference ranges in the lower band (percentile 10th).
- Medium scenario: Model and scenario whose DC difference ranges in the median of all projections.
- Upper scenario: Model and scenario whose DC difference ranges in the upper band (percentile 90th).

For example, the process of selection of the model and scenario for the Demonstration Area DA-01-IT has been the following:

***Table 6**. Selection of model and scenario to calculate future Lower, Medium and Upper scenarios for the DA-01-IT case of study.*

Model	Scenario	DC Difference	Centile
CanESM5	ssp245	-5.84	0
MRI-ESM2-0	ssp126	-2.78	3
MPI-ESM1-2-HR	ssp126	-2.73	6
ACCESS-CM2	ssp126	3.79	10
EC-EARTH3	ssp126	6.28	13
CMCC-ESM2	ssp245	11.02	17
CMCC-ESM2	ssp370	13.41	21
CMCC-ESM2	ssp126	19.04	25
CanESM5	ssp126	22.69	29
MPI-ESM1-2-HR	ssp370	48.03	34
CNRM-ESM2-1	ssp126	51.29	38
MPI-ESM1-2-HR	ssp245	66.11	42
EC-EARTH3	ssp370	71.21	46
ACCESS-CM2	ssp245	77.57	50
EC-EARTH3	ssp245	82.4	53
CNRM-ESM2-1	ssp370	94.65	57
MRI-ESM2-0	ssp370	99.07	61
EC-EARTH3	ssp585	99.23	64
MRI-ESM2-0	ssp245	99.69	68
CNRM-ESM2-1	ssp245	101.07	71
CMCC-ESM2	ssp585	106.16	75
ACCESS-CM2	ssp370	117.32	79
CanESM5	ssp370	119.11	83
MPI-ESM1-2-HR	ssp585	126.76	87

Copyright © FirEURisk Consortium. All rights reserved.

ACCESS-CM2	ssp585	135.16	90
MRI-ESM2-0	ssp585	138.78	93
CNRM-ESM2-1	ssp585	156.79	97
CanESM5	ssp585	185.13	100

In this case, the future projections of all variables will be calculated from the three selected scenarios: ACCESS-CM2 ssp126 obtained for the 9km x 9km grid will be used to calculate the Lower scenario in the case of study DA-01-IT, ACCESS-CM2 ssp245 will be used to calculate the Medium Scenario and the ACCESS-CM2 ssp585 to calculate the Upper Scenario.

This selection process is applied for each Pilot case or Demonstration area, obtaining a different model/ssp combination for each one of them.

4.2.2 Validation of results

Results obtained from the downscaling of 1km × 1km showed a few differences between the climate averages of, at most, 1°C in the case of maximum temperature. This difference in temperature may be caused by the differences in altitude between the two grids. However, the climate change signal of, for instance, 2071-2100 with respect 2021-2050, only is different in ±0.1°C for the 1km × 1km compared to 9km × 9km under the Medium scenario, while it is ±0.2°C under the Upper scenario.

In the case of precipitation, results show the same pattern as temperature: slight differences between both grids up to 10% due to the interpolation, but climate change signal remaining stable. In the example shown below, climate averages 2021-2050 are about 1.9mm/day and change between 2071-2100 and 2021-2050 lies around -2.1%, with minor differences between the two grids.

Copyright © FirEURisk Consortium. All rights reserved.

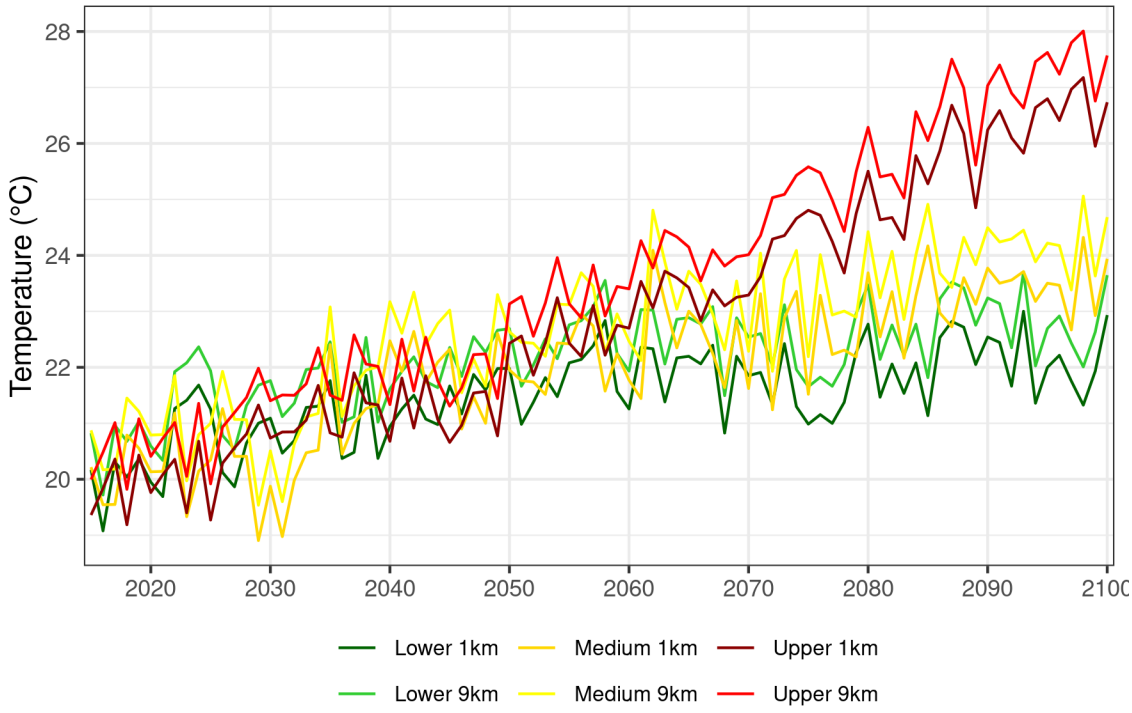


Figure 11: *Time series validation of Maximum Temperature for the case of study DA-01-IT (Sardinia, Italy) . Comparison between values obtained from the grids of 9km x 9km and 1km x 1km for the three scenarios: Lower, Medium and Upper.*

Copyright © FirEURisk Consortium. All rights reserved.

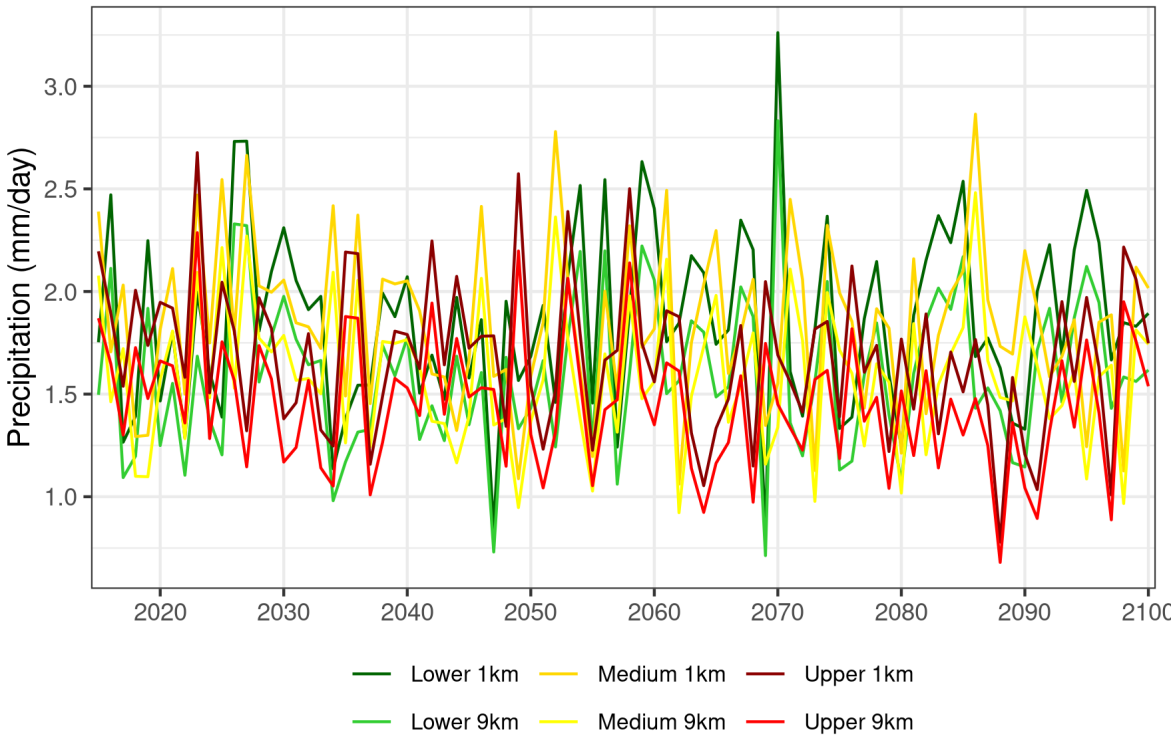


Figure 12: *Time series validation of Precipitation for the case of study DA-01-IT (Sardinia, Italy) . Comparison between values obtained from the grids of 9km x 9km and 1km x 1km for the three scenarios: Lower, Medium and Upper.*

Copyright © FirEURisk Consortium. All rights reserved.

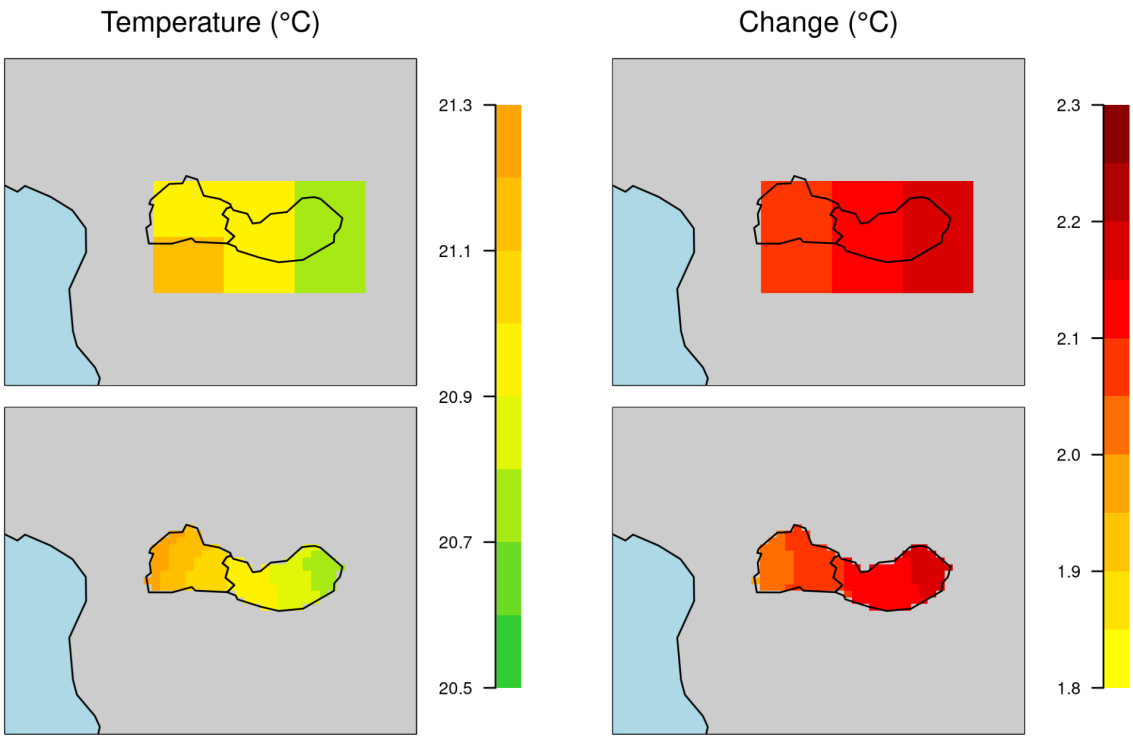


Figure 13: *Example of statistical downscaling result for DA-01-IT (Sardinia, Italy), for maximum temperature values (2021-2050 average) and change values of 2071-2100 compared to 2021-2050 period, before and after the second downscaling: 9km x 9km absolute values (upper left), 9km x 9km change values (upper right), 1km x 1km absolute values (bottom left), 1km x 1km change values (bottom right).*

Copyright © FirEURisk Consortium. All rights reserved.

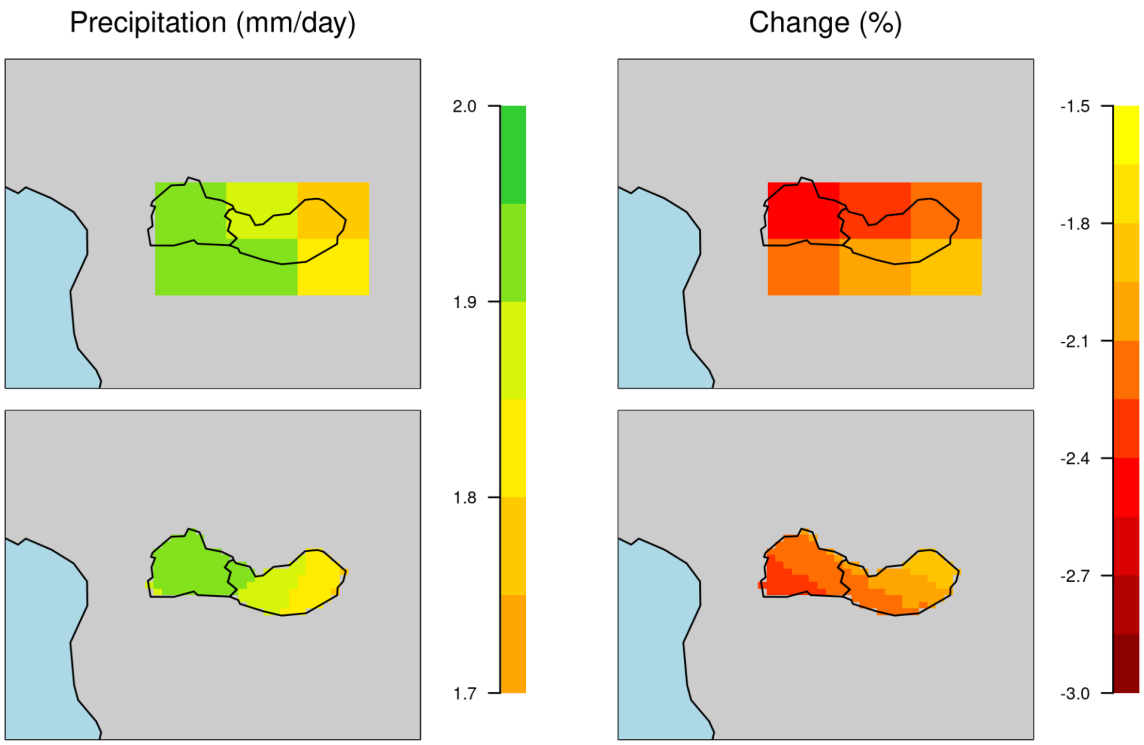


Figure 14: *Example of statistical downscaling result for DA-01-IT (Sardinia, Italy), for precipitation values (2021-2050 average) and change values of 2071-2100 compared to 2021-2050 period, before and after the second downscaling: 9km x 9km absolute values (upper left), 9km x 9km change values (upper right), 1km x 1km absolute values (bottom left), 1km x 1km change values (bottom right).*

4.3 CMIP5 contrast experiment in MED-Greece

4.3.1 Historical experiment (1980-2004 period)

Concerning the contrast experiment in MED-Greece, the downscaled CMIP5 EC-Earth/WRF showed good results on temperature, precipitation and humidity simulated under the *historical* experiment.

Various return periods (20, 50 and 100) of the examined climate variables and indices were calculated over the areas of interest for each grid point over the land grid cells for each period. Fire activity is the result of multiple, possibly interacting or correlated factors (weather conditions, topography, fuel moisture etc) acting at different scales. Identifying critical conditions is extremely important, taking into account that the relationships between index values and fire ignition and spread are non-linear (Wotton et al. 2009). For the estimation of the probability of occurrence we took into consideration certain thresholds of the variables that are associated with significant fire events, based on literature (Viegas 1998, Dimitrakopoulos et al. 2011, Athanasopoulou et al. 2014, Fernades et al 2016, Mitsopoulos et

Copyright © FirEURisk Consortium. All rights reserved.

al 2017, Field 2020), as follows for each variable: 1) maximum temperature >35 °C, 2) wind speed >8 m/s, 3) relative humidity < 30% and 4) SPI6< -1. The results are illustrated in figures 3 to 11 and the most noticeable results are summarised in the following lines. Overall, the results provide an assessment of the regional potential of the demonstration and pilot areas for extreme fire weather conditions.

Firstly, Figures from 3 to 6 illustrate the values of return periods for the examined variables in the historical period.

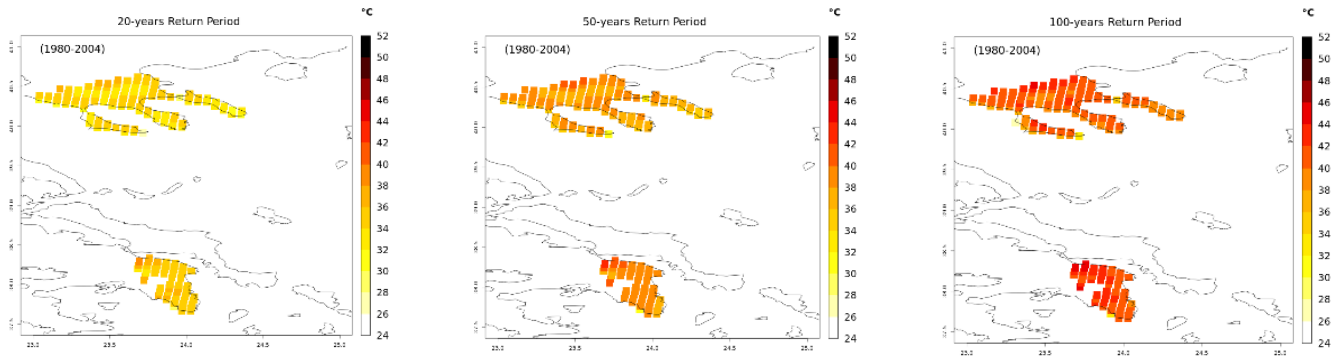


Figure 15. *Maximum temperature's values of 20-years return period (left), 50-years return period (centre) and 100-years return period (right) for the historical period 1980-2004 in the DA and PS.*

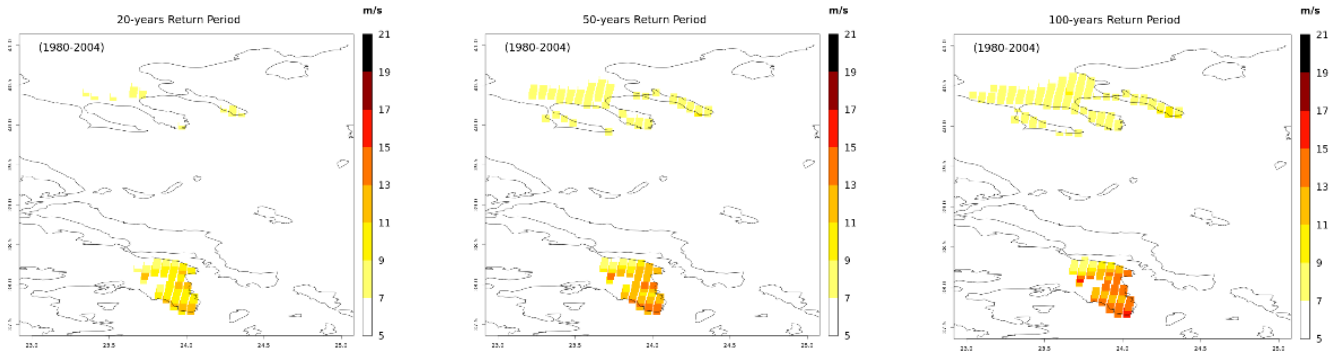


Figure 16. *Wind speed's values of 20-years return period (left), 50-years return period (centre) and 100-years (right) return period for the historical period 1980-2004 in the DA and PS.*

Copyright © FirEURisk Consortium. All rights reserved.

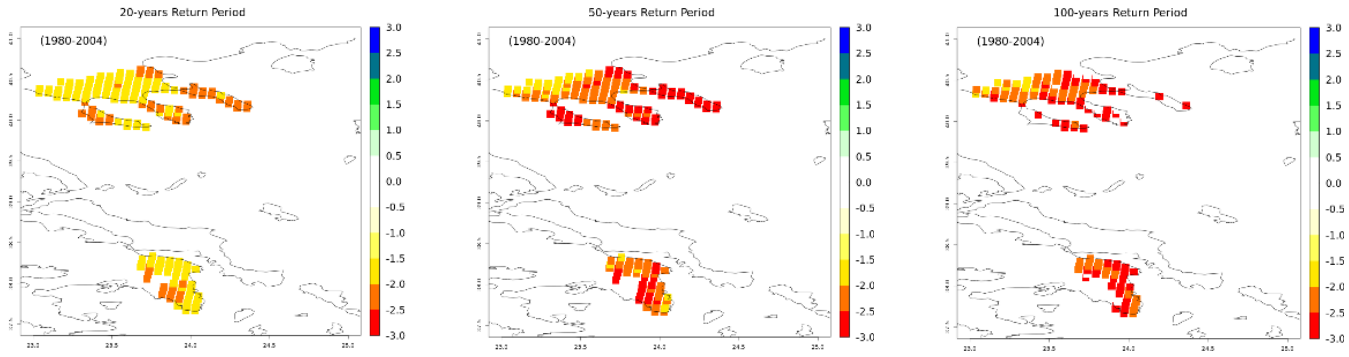


Figure 17. *SPI6's values of 20-years return period (left), 50-years return period (centre) and 100-years (right) return period for the historical period 1980-2004 in the DA and PS.*

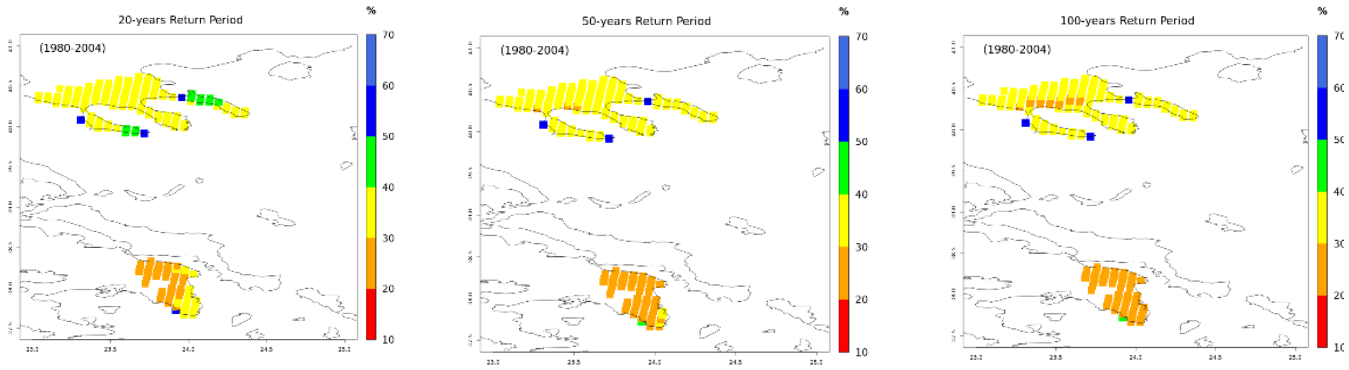


Figure 18. *Relative humidity's values of 20-years return period (left), 50-years return period (centre) and 100-years (right) return period for the historical period 1980-2004 in the DA and PS.*

As a summary, results for the historical period showed that:

- From 32°C to 38°C for 20-year return period, increasing temperature for 50 and 100 years return period with values yielding up to 44 degrees based on the historical period for both areas.
- Wind speed increases progressively from 7 m/s and 15 m/s to 17 m/s, for 20,50 and 100 years return period, particularly in the study area of East Attica Region for the historical period
- Drier conditions increase (with extreme drought values of SPI6, below -2) from 20 to 100 years return period for both pilot study areas.

Regarding the climate change projections, results are synthesised here:

- Concerning maximum temperature and wind speed, the values of return periods do not mark noticeable differences among different RCP's scenarios and periods (near or far), only between different return periods. On the other hand, the return values of SPI6 yield different performance and for RCPs

Copyright © FirEURisk Consortium. All rights reserved.

- East Attica Region will face drier conditions (lower negative values of SPI6) under RCP 4.5 and for 50- and 100 years return period, while Chalkidiki under RCP8.5.
- Overall, relative humidity is lower in the near future period and under both scenarios, particularly in the East Attica Region, than in the far future.
- For maximum temperature, the probability of exceeding the threshold of 35 degrees Celsius increases notably in the late future and under RCP8.5, with higher probability values for East Attica Region.
- The probability of occurrence of wind speed above 8 m/s is similarly increasing under both scenarios and periods, with maximum peak in specific areas of East Attica Region. Slightly increasing probability values are observed in central Chalkidiki.
- Greater values of probability of exceedance of spi6<-1, indicating drier conditions, are noticed in the demonstrate areas of Chalkidiki for both periods and RCPs, while East Attica Region yields higher probability values under RCP4.5. Under RCP8.5, only the northern and southern parts of East Attica Region (which are characterised by significant vegetation) marked higher probability of facing important drier conditions.
- Greater values of the probability of relative humidity to exceed the threshold of 30% is observed for both areas in the near future period and under both scenarios.

Overall, the increase of drought conditions (due to lower relative humidity of lack of precipitation) and rising temperatures, combined with higher wind speed can lead to a prolonged fire season in the future, starting earlier in the spring and ending later in the fall. Also, higher temperatures dry out vegetation, making it more prone to burning. More details can be found in the Annex (Figures 7 to 10), which depicts the expected values of return periods under the two periods and the two scenarios. The results of probability of occurrence above a certain threshold is illustrated in Figure 11 under RCP4.5 and RCP8.5. The fire danger is expected to progressively increase in the future especially in the high-end climate change.

4.4 Documentation of results

Products are available with OpenData service at gitlab.meteogrid.com/public-access/fireurisk. A summary of parameters to select NetCDF is shown below:

- **List of variables produced:** TMax; TMin; HRMax **; HRMin **; tpr; u10m; v10m; windspeed; LWR; SWR. ** Not available for the following models: BCC-CSM2-MR, NorESM2-MM and UKESM1-0-LL
- **List of calendars:** (1) Proleptic gregorian; (2) 365-day (excludes February 29th); (3) 360-day (12 months of 30 days**)**
- **List of models (and calendar)**: ACCESS-CM2 (1); BCC-CSM2-MR (2); CanESM5 (2); CMCC-ESM2 (2); CNRM-ESM2-1 (1); EC-EARTH3 (1); MPI-ESM1-2-HR (1); MRI-ESM2-0 (1); NorESM2-MM (2); UKESM1-0-LL (3)

An easy Python code can be built to manage the data and apply it as an input for any environmental model. For instance:

```
import datetime as dt  # Python standard library datetime  module
import numpy as np
import matplotlib.pyplot as plt
from netCDF4 import Dataset
```

Copyright © FirEURisk Consortium. All rights reserved.

```
url = 'https://niebla.ficlima.org/thredds/dodsC/Fireurisk/ACCESS-CM2/TMax/TMax_ACCESS-CM2_ssp245.nc'
f = Dataset(url, "r", format="NETCDF4")

# Uploading all the required libraries
print(f.history)
print(f.dimensions)
print(f.variables)
print(f.variables.keys())
variable = list(f.variables.keys())[3]

# Reading the time and spatial references as well as copying the interest variable in an array
time = f.variables['time'][:].copy()
time_units = f.variables['time'].units
lats = f.variables['lat'][:].copy()
lons = f.variables['lon'][:].copy()
arr = f.variables[variable][:,:,0].copy()

# Showing the data just to check it
plt.imshow(arr)
plt.show()

# Plotting the figure as you desire. For instance, the countorns for each Celsius Degree, ranged between -25 and 32.
fig = plt.figure(figsize=(14,10))
ax = fig.add_subplot(2, 2, 4)
p = plt.contourf(lons, lats, arr, cmap = plt.cm.get_cmap('jet'), levels=np.arange(-25, 32, 1))
fig.colorbar(p)
```

5 Conclusions

The downscaled model outputs showed a good performance for both 9km and 1km resolution grid. Particularly, taking each reanalysis grid point (9km resolution) as a reference, it has been possible to downscale the entire projected daily series (without forcing the seasonal variability) of all the models and scenarios for all the climate variables necessary to determine fire risk. After this, the seasonal cycle over the year presented a good performance for all the cases and the average errors for the 9km resolution grid were less than 1°C in the case of temperature and less than 3% in the case of precipitation.

Once obtained and validated the climate variables for the 9km resolution grid, three representative future scenarios were selected for each PS and DA according to their differences of Drought Code. Then, all the climate variables of those scenarios were downscaled to a 1km grid resolution for each area. Validations for the case of study DA-01-IT (Sardinia, Italy), show that differences between both grids are minor and possibly due to the altitude correction. In any case, these differences do not affect the future climate change signal, which remains unchanged.

Copyright © FirEURisk Consortium. All rights reserved.

Concerning the contrast experiment in MED-Greece, the increase of drought conditions (due to lower relative humidity of lack of precipitation) and rising temperatures, combined with higher wind speed can lead to a prolonged fire season in the future, starting earlier in the spring and ending later in the fall.

6 References

Benestad RE (2010) Theor Appl Climatol 100: 1–21. 10.1007/s00704-009-0158-1

Bentsen, M.; Oliviè, D. J. L.; Seland, Ø. et al. (2019). NCC NorESM2-MM model output prepared for CMIP6 ScenarioMIP. Earth System Grid Federation. doi: 10.22033/ESGF/CMIP6.608.

Brun, P., Zimmermann, N. E., Hari, C., Pellissier, L., and Karger, D. N. (2022): Global climate-related predictors at kilometre resolution for the past and future, Earth Syst. Sci. Data Discuss. [preprint], doi:10.5194/essd-2022-212.

Chylek P, Li J, Dubey M, Wang M, Lesins G. (2011). Observed and model simulated 20th century Arctic temperature variability: Canadian Earth System Model CanESM2. Atmos. Chem. Phys. Discuss. 11: 22893–22907. doi:10.5194/acpd-11- 22893-2011.

Collins W, Bellouin N, Doutriaux-Boucher M, Gedney N, Hinton T, Jones CD, Liddicoat S, Martin G, O'Connor F, Rae J, Senior C, Totterdell I, Woodward S, Reichler T, Kim J, Halloran P. (2008). Evaluation of the HadGEM2 model. Hadley Centre Technical Note. HCTN 74, Met Office Hadley Centre, Exeter, UK.

Copernicus-C3S (2020): High-resolution climate projections. Climate Data Factory. Website link: https://climate.copernicus.eu/high-resolution-climate-projections

Copernicus-C3S (2022). Climadjust, a Bias-Adjustment service for the Climate Data Store. Website link: https://climate.copernicus.eu/climadjust-bias-adjustment-service-climate-data-store

Dunne J. P. et al. (2012). GFDL's ESM2 Global Coupled Climate–Carbon Earth System Models. Part I: Physical Formulation and Baseline Simulation Characteristics. J. Climate, 25, 6646–6665, doi:10.1175/JCLI-D-11-00560.1.

EC-Earth Consortium (EC-Earth) (2019). EC-Earth-Consortium EC-Earth3-Veg model output prepared for CMIP6 Scenario MIP. Earth System Grid Federation, doi:10.22033/ESGF/CMIP6.727. Data doi:10.24381/cds.c866074c.

EURO-CORDEX (2022). Euro-CORDEX Website link: https://www.euro-cordex.net/060374/index.php.en

Eyring, V., Bony, S., Meehl, G. A., Senior, C. A., Stevens, B., Stouffer, R. J., and Taylor, K. E. (2016). Overview of the Coupled Model Intercomparison Project Phase 6 (CMIP6) experimental design and organization, Geosci. Model Dev. 9: 1937-1958. doi:10.5194/gmd-9-1937-2016.

Good P., Sellar A., Tang Y., Rumbold S., Ellis R., Kelley D., Kuhlbrodt T. (2019). *MOHC UKESM1.0-LL model output prepared for CMIP6 ScenarioMIP ssp245*. Earth System Grid Federation. doi:10.22033/ESGF/CMIP6.6339.

Iversen T, Bentsen M, Bethke I, Debernard JB, Kirkevag A, Seland O, et al. The Norwegian Earth System Model, NorESM1-M - Part 2: Climate response and scenario projections. Geoscientific Model Development 2013; 6: 389-415.

Krasting, J. P.; John, J. G; Blanton, C. et al. (2018). NOAA-GFDL GFDL-ESM4 model output prepared for CMIP6 CMIP. Earth System Grid Federation. doi:10.22033/ESGF/CMIP6.1407.

Marsland SJ, Haak H, Jungclaus JH, Latif M, Roske F (2013). The Max-Planck-Institute global ocean/sea ice model with orthogonal curvilinear coordinates. Ocean Modelling 5: 91-127.

Copyright © FirEUrisk Consortium. All rights reserved.

Monjo R., Caselles V., Chust G. (2014). Probabilistic correction of RCM precipitation in the Basque Country (Northern Spain). Theoretical and Applied Climatology, 117: 317-329. doi: 10.1007/s00704-013-1008-8.

Monjo, R.; Gaitán, E.; Pórtoles, J.; Ribalaygua, J.; Torres, L. (2016): Changes in extreme precipitation over Spain using statistical downscaling of CMIP5 projections. International Journal of Climatology, 36: 757-769. DOI: 10.1002/joc.4380.

Ribalaygua J, Torres L, Pórtoles J, Monjo R, Gaitán E, Pino MR. (2013). Description and validation of a two-step analogue/regression downscaling method. Theoretical and Applied Climatology, 114: 253-269. doi:10.1007/s00704-013-0836-x.

Seferian R. (2019). CNRM-CERFACS CNRM-ESM2-1 model output prepared for CMIP6 AerChemMIP hist-1950HC. Version YYYYMMDD[1].Earth System Grid Federation. doi:10.22033/ESGF/CMIP6.4041.

Swart N. C., Cole J. N. S., Kharin V. V., Lazare M., Scinocca J. F., Gillett N. P., Anstey J., Arora V., Christian J. R., Hanna S., Jiao Y., Lee W. G., Majaess F., Saenko O. A., Seiler C., Seinen C., Shao, A., Sigmond M., Solheim L., von Salzen K., Yang D. and Winter B. (2019). The Canadian Earth System Model version 5 (CanESM5.0.3), Geosci. Model Dev., 12, 4823–4873, doi:10.5194/gmd-12-4823-2019.

Voldoire A, Sanchez-Gomez E, Melia DSY, Decharme B, Cassou C, Senesi S, et al. (2013). The CNRM-CM5.1 global climate model: description and basic evaluation. Climate Dynamics 40: 2091-2121.

Von Storch, J.-S.; Putrasahan, D.; Lohmann, K. et al. (2017). MPI-M MPIESM1.2-HR model output prepared for CMIP6 HighResMIP. Earth System Grid Federation. doi: 10.22033/ESGF/CMIP6.762.

Watanabe S, Hajima T, Sudo K, Nagashima T, Takemura T, Okajima H, et al. MIROC-ESM 2010: model description and basic results of CMIP5-20c3m experiments. Geoscientific Model Development 2011; 4: 845-872.

Wu T., Lu Y., Fang Y., Xin X., Li L., Li W., Jie W., Zhang J., Liu Y., Zhang L., Zhang F., Zhang Y., Wu F., Li J., Chu M., Wang Z., Shi X., Liu X., Wei M., Huang A., Zhang Y. and Liu, X. (2019). The Beijing Climate Center Climate System Model (BCC-CSM): the main progress from CMIP5 to CMIP6 , Geosci. Model Dev. 12, 1573–1600. doi:10.5194/gmd-12-1573-2019, 2019.

Xiao-Ge X, Tong-Wen W, Jie Z. Introduction of CMIP5 experiments carried out with the climate system models of Beijing Climate Center. Adv. Clim. Chang. Res. 2013; 4:41–49. doi: doi.org/10.3724/SP.J.1248.2013.041.

Yukimoto S., Koshiro T., Kawai H., Oshima N., Yoshida, K., Urakawa S.; Tsujino H., Deushi M., Tanaka T., Hosaka M., Yoshimura H., Shindo E., Mizuta R., Ishii M., Obata A., Adachi, Y. (2019). MRI MRI-ESM2.0 model output prepared for CMIP6 CMIP. Earth System Grid Federation. doi:10.22033/ESGF/CMIP6.621.

Ziehn T., Chamberlain M., Lenton A., Law R., Bodman R., Dix M., Wang Y., Dobrohotoff P., Srbinovsky J., Stevens L., Vohralik P., Mackallah C, Sullivan A., O'Farrell S., Druken K. (2019). CSIRO ACCESS-ESM1.5 model output prepared for CMIP6 CMIP. Earth System Grid Federation. doi:10.22033/ESGF/CMIP6.2288.

Copyright © FirEURisk Consortium. All rights reserved.

7 Annex A: Climate scenarios of the MED-Greece experiments

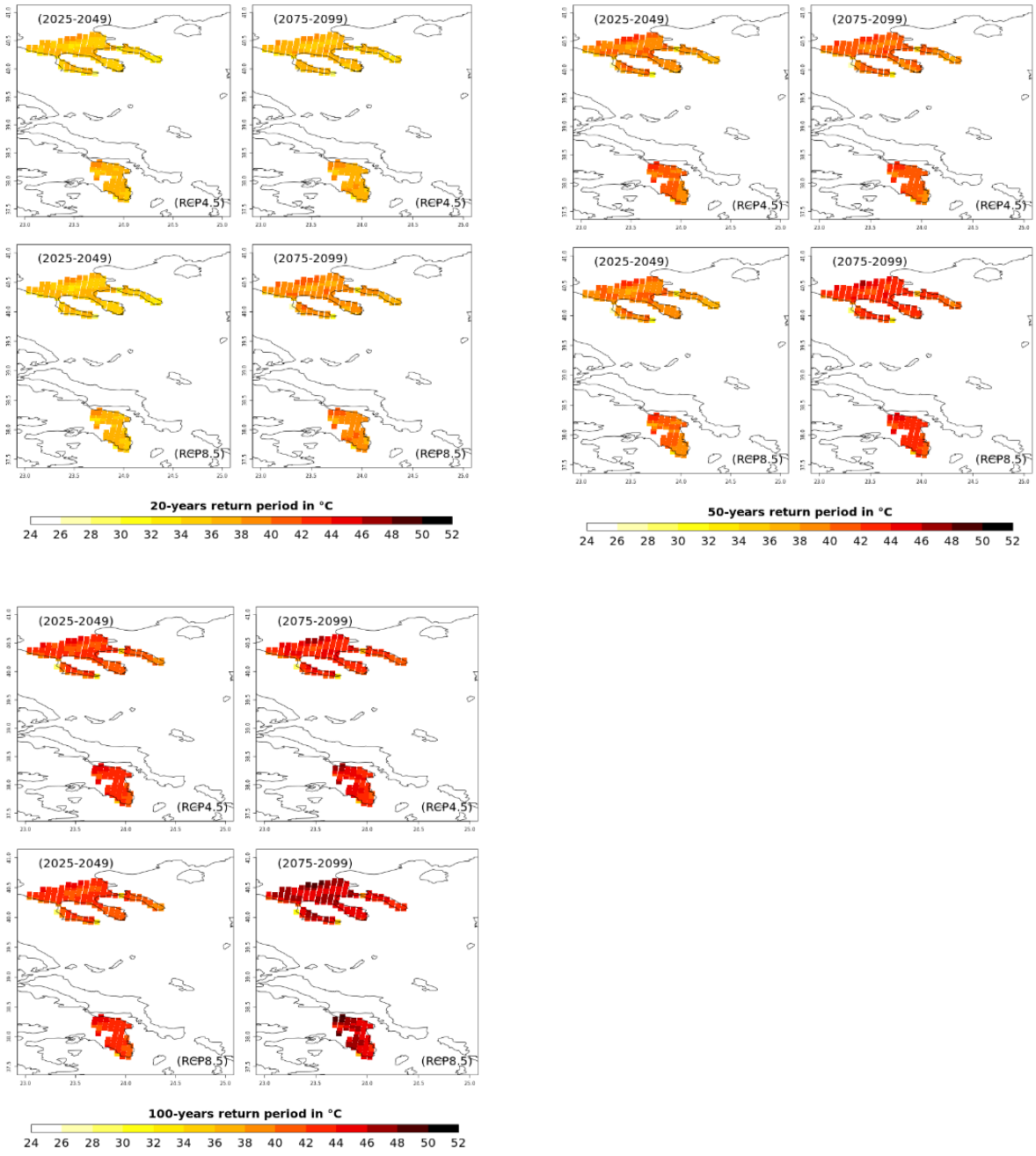


Figure 19. *Maximum Temperature's values of 20-years return period (upper left), 50-years return period (upper right) and 100-years return period (below) for the near and far future period under RCP4.5 and RCP8.5 in the DA and PS.*

Copyright © FirEURisk Consortium. All rights reserved.

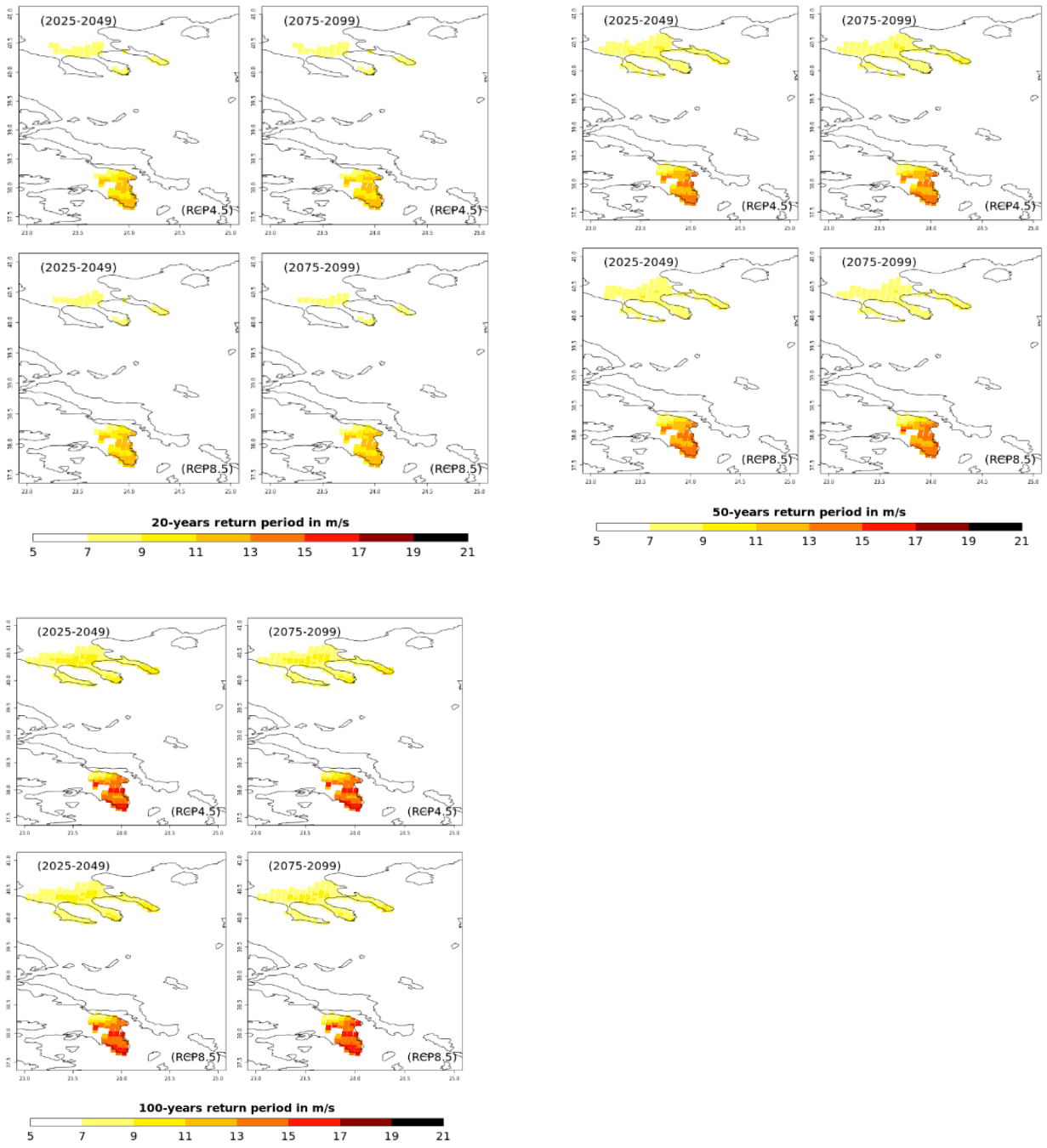


Figure 20. *Wind speed's values of 20-years return period (upper left), 50-years return period (upper right) and 100-years return period (below) for the near and far future period under RCP4.5 and RCP8.5 in the DA and PS.*

Copyright © FirEURisk Consortium. All rights reserved.

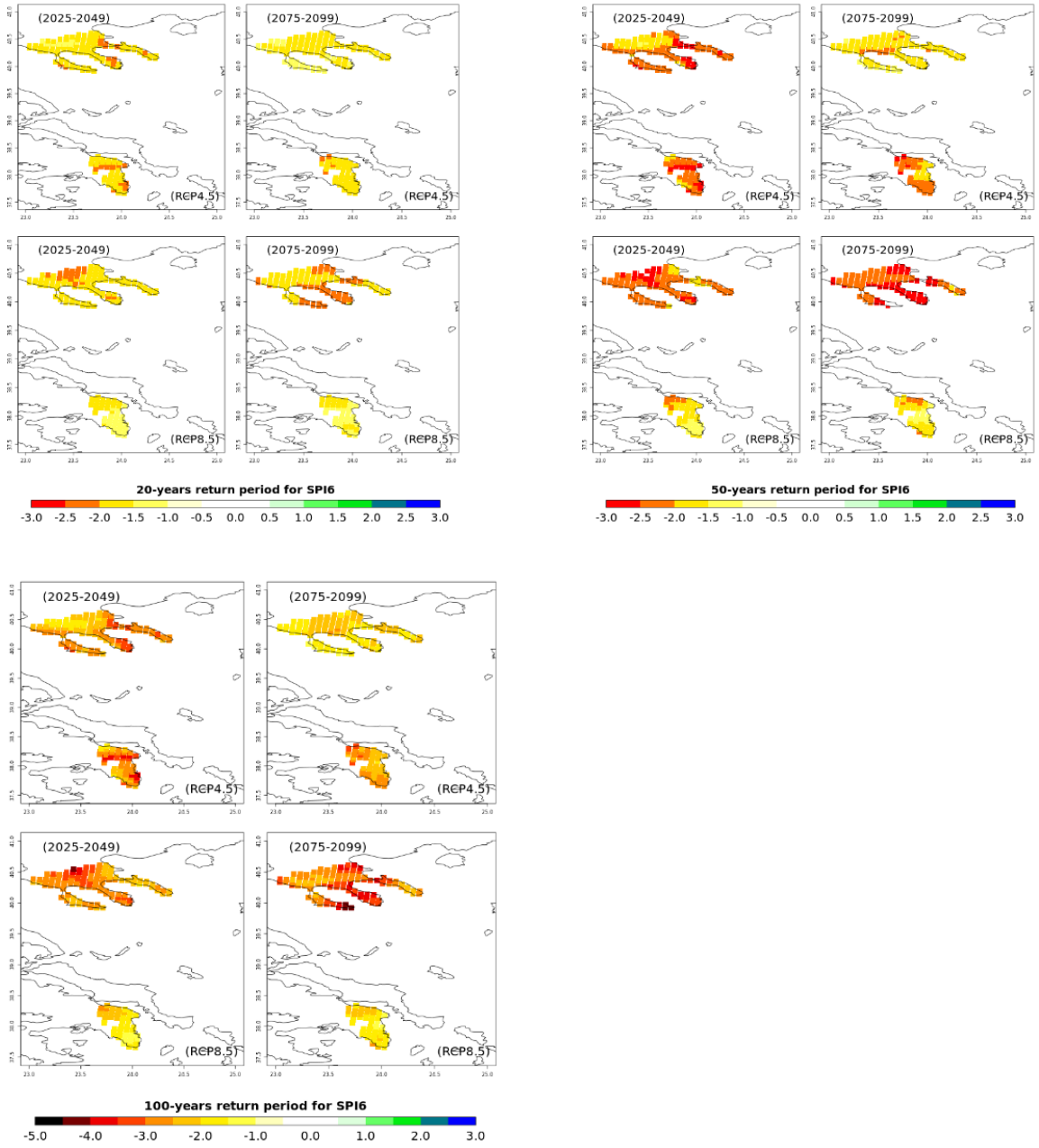


Figure 21. *SPI6's values of 20-years return period (upper left), 50-years return period (upper right) and 100-years return period (below) for the near and far future period under RCP4.5 and RCP8.5 in the DA and PS.*

Copyright © FirEURisk Consortium. All rights reserved.

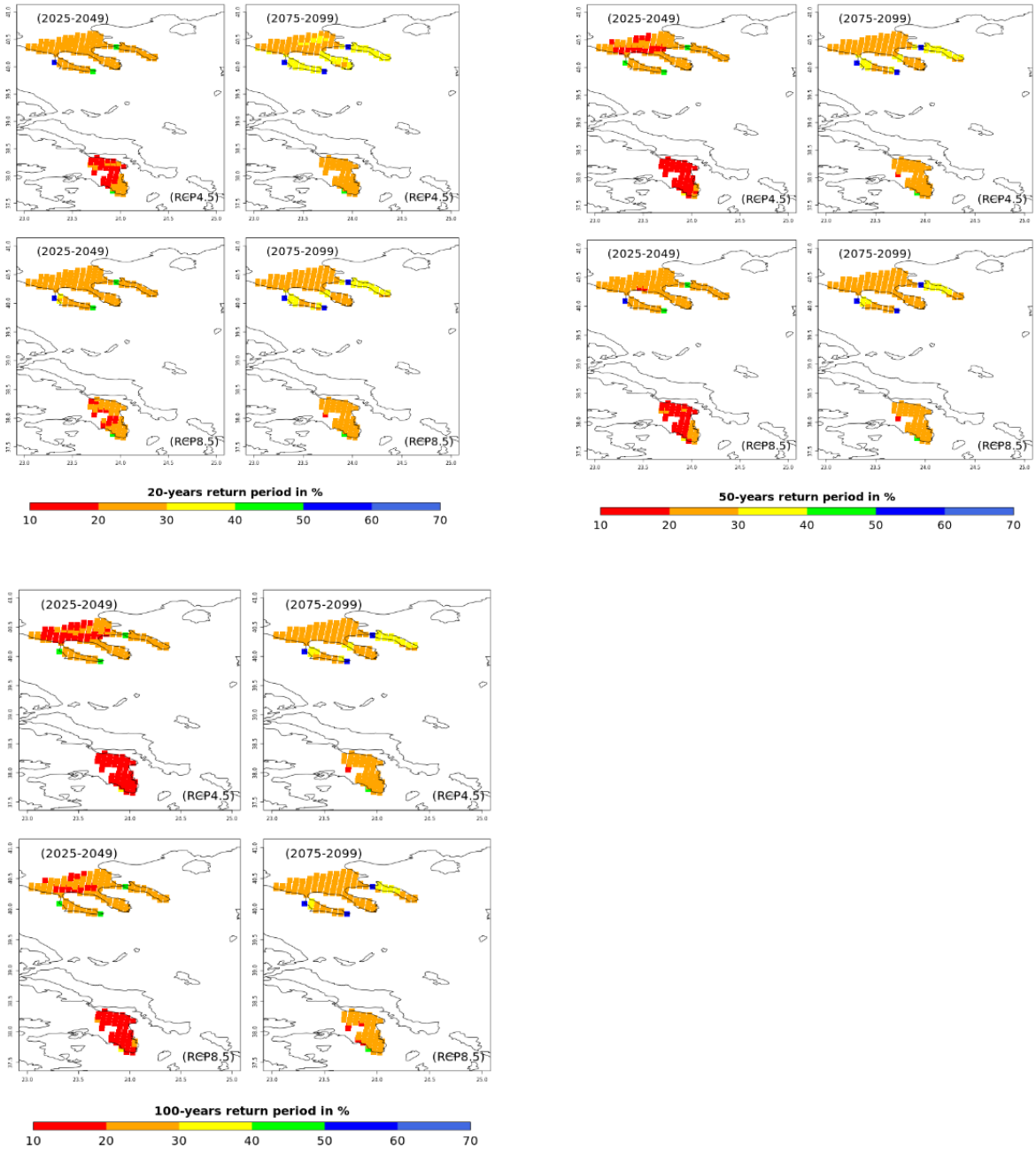


Figure 22. *Relative humidity's values of 20-years return period (upper left), 50-years return period (upper right) and 100-years return period (below) for the near and far future period under RCP4.5 and RCP8.5 in the DA and PS.*

Copyright © FirEURisk Consortium. All rights reserved.

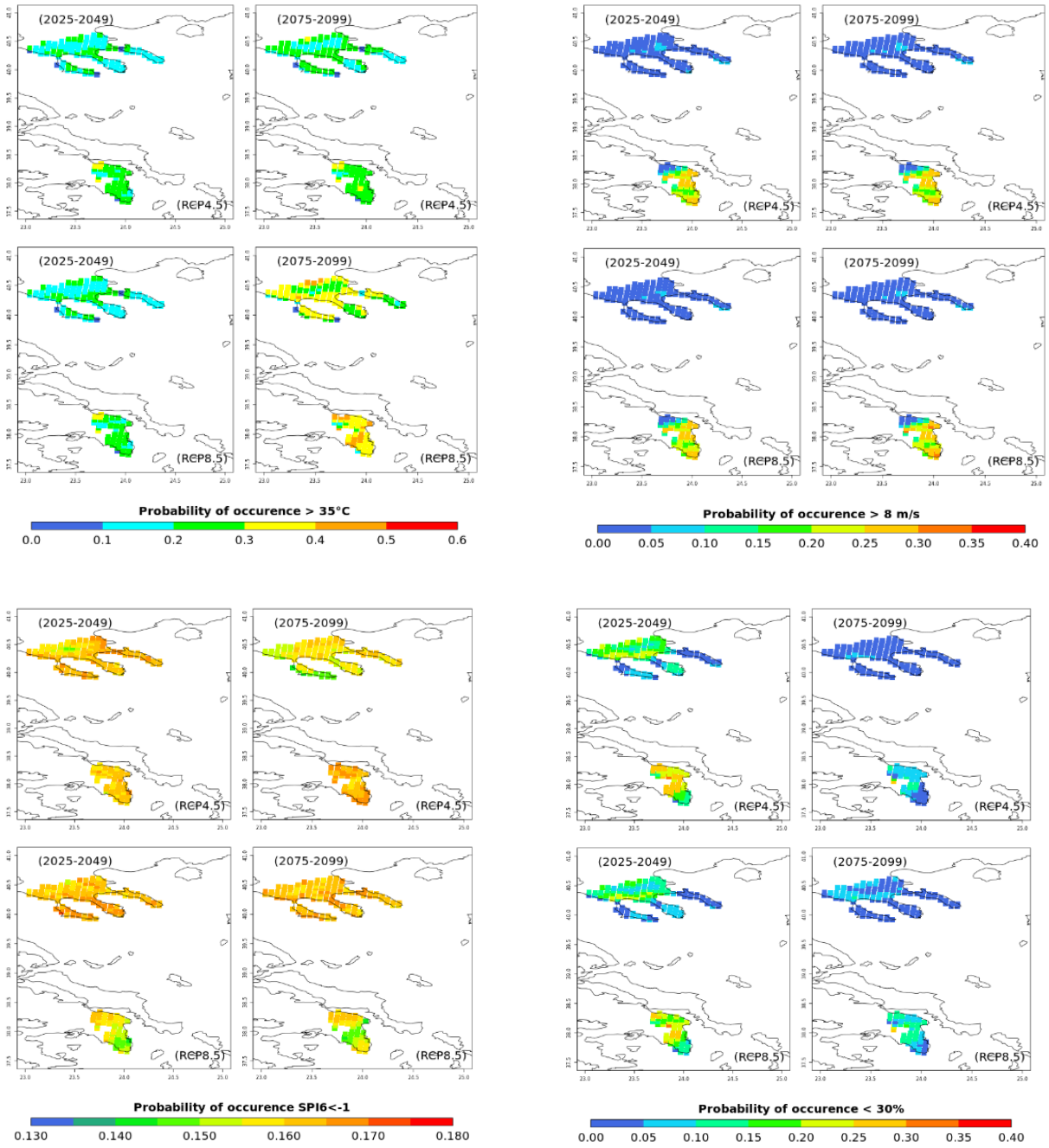


Figure 23. *Probability of exceeding a threshold for maximum temperature>35°C (upper left), wind speed>8m/s (upper right), SPI6<-1 (bottom left) and relative humidity<30% (bottom right) for the far and future periods under RCP4.5 and RCP8.5.*

Copyright © FirEURisk Consortium. All rights reserved.

Annex B: Selection of climate models and scenarios

Table 7. Selection of model and scenario to calculate future Lower, Medium and Upper scenarios for the whole 9km x 9km European grid.

Model	Scenario	DC Difference
CanESM5	ssp245	4.36
CMCC-ESM2	ssp370	46.68
CanESM5	ssp585	75.01

Table 8. Selection of model and scenario to calculate future Lower, Medium and Upper scenarios for each case of study.

Case of study	Lower scenario	Medium scenario	Upper scenario
DA-01-IT	ACCESS-CM2_ssp126	ACCESS-CM2_ssp245	ACCESS-CM2_ssp585
DA-02-IT	ACCESS-CM2_ssp126	ACCESS-CM2_ssp245	MRI-ESM2-0_ssp585
DA-03-IT	ACCESS-CM2_ssp126	EC-EARTH3_ssp245	MPI-ESM1-2-HR_ssp245
DA-04-IT	ACCESS-CM2_ssp126	EC-EARTH3_ssp585	MRI-ESM2-0_ssp585
DA-05-IT	ACCESS-CM2_ssp126	EC-EARTH3_ssp245	MPI-ESM1-2-HR_ssp585
DA-06-IT	CanESM5_ssp126	CMCC-ESM2_ssp585	MRI-ESM2-0_ssp585
DA-07-IT	EC-EARTH3_ssp126	MPI-ESM1-2-HR_ssp245	MPI-ESM1-2-HR_ssp585
DA-08-IT	CMCC-ESM2_ssp245	ACCESS-CM2_ssp370	MRI-ESM2-0_ssp585
DA-09-IT	EC-EARTH3_ssp126	ACCESS-CM2_ssp245	CanESM5_ssp585
DA-10-FR	CMCC-ESM2_ssp245	MPI-ESM1-2-HR_ssp245	EC-EARTH3_ssp585
DA-11-FR	MRI-ESM2-0_ssp126	CNRM-ESM2-1_ssp370	CNRM-ESM2-1_ssp585

Copyright © FirEURisk Consortium. All rights reserved.

DA-12-FR	CanESM5_ssp245	CNRM-ESM2-1_ssp370	CMCC-ESM2_ssp585
DA-13-FR	EC-EARTH3_ssp126	CNRM-ESM2-1_ssp370	CMCC-ESM2_ssp585
DA-14-UK	EC-EARTH3_ssp126	MPI-ESM1-2-HR_ssp370	CanESM5_ssp585
DA-15-UA	ACCESS-CM2_ssp126	CMCC-ESM2_ssp585	EC-EARTH3_ssp370
DA-16-SE	EC-EARTH3_ssp126	EC-EARTH3_ssp585	ACCESS-CM2_ssp370
DA-17_Castells	CanESM5_ssp126	ACCESS-CM2_ssp245	CNRM-ESM2-1_ssp585
DA-17_Morella	CanESM5_ssp126	ACCESS-CM2_ssp245	CNRM-ESM2-1_ssp585
DA-19-ES	CanESM5_ssp126	MRI-ESM2-0_ssp370	CanESM5_ssp370
DA-20-HR	CNRM-ESM2-1_ssp126	CNRM-ESM2-1_ssp245	MPI-ESM1-2-HR_ssp585
DA-21-PT	MRI-ESM2-0_ssp126	ACCESS-CM2_ssp370	EC-EARTH3_ssp585
DA-22-PT	CanESM5_ssp126	ACCESS-CM2_ssp370	MPI-ESM1-2-HR_ssp585
DA-23-EL	MRI-ESM2-0_ssp126	CNRM-ESM2-1_ssp126	CNRM-ESM2-1_ssp370
DA-24-EL	MRI-ESM2-0_ssp126	MPI-ESM1-2-HR_ssp245	ACCESS-CM2_ssp585
DA-25-CZ	CanESM5_ssp245	MRI-ESM2-0_ssp585	ACCESS-CM2_ssp370
DA-26-RO	CNRM-ESM2-1_ssp126	CMCC-ESM2_ssp245	EC-EARTH3_ssp585
PS-01-SE	EC-EARTH3_ssp126	EC-EARTH3_ssp585	ACCESS-CM2_ssp370
PS-02-DE.CZ.PL	MRI-ESM2-0_ssp245	MRI-ESM2-0_ssp585	CMCC-ESM2_ssp585
PS-03-PT	MRI-ESM2-0_ssp126	ACCESS-CM2_ssp370	CMCC-ESM2_ssp370
PS-04-ES	CanESM5_ssp245	MRI-ESM2-0_ssp245	MPI-ESM1-2-HR_ssp585
PS-05-EL	ACCESS-CM2_ssp126	CNRM-ESM2-1_ssp126	MPI-ESM1-2-HR_ssp585

Copyright © FirEURisk Consortium. All rights reserved.